AD NUMBER

AD840127

LIMITATION CHANGES

TO:

Approved for public release; distribution is unlimited.

FROM:

Distribution: Further dissemination only as directed by Space and Missile Systems Organization, Los Angeles, CA 90045, SEP 1968, or higher DoD authority.

AUTHORITY

SAMSO ltr 16 Aug 1973

AEDC-TR-68-203

cy 1

STEADY AND FLUCTUATING PRESSURES AROUND FLOW PROTUBERANCES ON THE MOL VEHICLE AT TRANSONIC SPEEDS

R. W. Butler and J. F. Riddell

ARO, Inc.

September 1968

PROPULSION WIND TUNNEL FACILITY
ARNOLD ENGINEERING DEVELOPMENT CENTER
AIR FORCE SYSTEMS COMMAND
ARNOLD AIR FORCE STATION, TENNESSEE

NOTICES

When U. S. Government drawings specifications, or other data are used for any purpose other than a definitely related Government procurement operation, the Government thereby incurs no responsibility nor any obligation whatsoever, and the fact that the Government may have formulated, furnished, or in any way supplied the said drawings, specifications, or other data, is not to be regarded by implication or otherwise, or in any manner licensing the holder or any other person or corporation, or conveying any rights or permission to manufacture, use, or sell any patented invention that may in any way be related thereto.

Qualified users may obtain copies of this report from the Defense Documentation Center.

References to named commercial products in this report are not to be considered in any sense as an endorsement of the product by the United States Air Force or the Government.

STEADY AND FLUCTUATING PRESSURES AROUND FLOW PROTUBERANCES ON THE MOL VEHICLE AT TRANSONIC SPEEDS

R. W. Butler and J. F. Riddell

ARO, Inc.

This document has been approved for public release [illegible] its distribution is unlimited.

FOREWORD

The work reported herein was done at the request of the Space and Missile Systems Organization (SAMSO), Air Force Systems Command (AFSC), for the McDonnell-Douglas Corporation, Huntington Beach, California, under Program Element 6340940F/632A.

The results of the test presented were obtained by ARO, Inc. (a subsidiary of Sverdrup & Parcel and Associates, Inc.) contract operator of the Arnold Engineering Development Center (AEDC), AFSC, Arnold Air Force Station, Tennessee, under Contract F40600-69-C-0001. This test was conducted from July 2 to 9, 1968, under ARO Project No. PB0895, and the manuscript was submitted for publication on August 20, 1968.

This technical report has been reviewed and is approved.

Richard W. Bradley
Lt Colonel, USAF
AF Representative, PWT
Directorate of Test

Roy R. Croy, Jr.
Colonel, USAF
Director of Test

ABSTRACT

A wind tunnel investigation was conducted in the Propulsion Wind Tunnel, Transonic (16T) to obtain steady and fluctuating pressures to assess the aerodynamic effects on the local and downstream flow fields caused by large protuberances on the Manned Orbital Laboratory (MOL) vehicle. Pressure data were recorded at Mach numbers 0.80, 0.90, 1.10, 1.20, 1.40, and 1.55 for angles of attack of -7.5, 0, and 4 deg and angles of sideslip of -6 and 6 deg. Test results revealed that the left- and right-side auxiliary-equipment fairings and their afterbodies do not impose a significant interference effect on each other, whereas the horizon-sensor-fairing and auxiliary-equipment-fairing flow interaction attributes up to 50 percent of the pressure fluctuations at selected microphone locations. Of the four base configurations on the auxiliary-equipment fairings, the 10-deg conical afterbody exhibited the lowest overall dynamic-pressure level at all test conditions.

CONTENTS

APPENDIXES

I. ILLUSTRATIONS

Figure

NOMENCLATURE

C_p	Local pressure coefficient, $(p_L - p_\infty)/q_\infty$
M_∞	Free-stream Mach number
p_L	Local static pressure, psf
p_{RMS}	Root-mean-square (rms) pressure fluctuations, psf
p_{RMS}/p_L	Dynamic-pressure ratio
p_{t_∞}	Free-stream total pressure, psf
p_∞	Free-stream static pressure, psf
q_∞	Free-stream dynamic pressure, psf
Re/ft	Reynolds number per foot
α_m	Angle of attack, deg
β	Angle of sideslip, deg
ϕ	Roll angle, deg

SECTION I
INTRODUCTION

Pressure fluctuations on the Manned Orbital Laboratory (MOL) vehicle caused by the turbulent boundary layer and separated flows around flow-perturbing geometries are required to evaluate the structural integrity of the vehicle. These fluctuating pressures contribute to the fatigue of the structure and possible failure of equipment susceptible to vibration or acoustic pressures. In order to determine the effects of some aerodynamic factors and certain geometries on fluctuating pressures, rigid-model wind tunnel tests are used to define in-flight fluctuating pressures at the walls of the vehicle.

Specific controlled experiments in the Propulsion Wind Tunnel, Transonic (16T), were run to define the aerodynamic effects of flow-perturbing geometries on the local and downstream flow fields.

Both steady- and unsteady-pressure measurements were obtained for four model configurations. Results are presented in terms of dynamic-pressure ratio defined as the root-mean-square (rms) pressure fluctuation normalized by model local static pressure.

SECTION II
APPARATUS

2.1 TEST FACILITY

Tunnel 16T is a continuous flow, closed-circuit wind tunnel capable of operating at Mach numbers from 0.55 to 1.60. Stagnation pressure ranges from approximately 160 to 4000 psfa with a maximum stagnation temperature of 120°F. The removable test section is 16 ft square and 40 ft long with 6-percent-open perforated test section walls which allow continuous operation throughout the Mach number range. A sketch of the test section wall details and the location of the test model in the test section is shown in Fig. 1, Appendix I. A more thorough description of the tunnel may be found in Ref. 1, and applicable calibration results are presented in Refs. 2 and 3.

2.2 TEST ARTICLE

The MOL rigid body fluctuating pressure model is a 10-percent-scale model of the MOL vehicle. The model consists of the Gemini "B" capsule,

the laboratory module, and a portion of the mission module. A sketch of the basic model is shown in Fig. 2. A photograph showing the model installed in Tunnel 16T is shown in Fig. 3.

Protuberances mounted on the model during the wind tunnel investigation were a fin, thruster modules, a mission-module fairing, a left-side auxiliary-equipment fairing, a right-side auxiliary-equipment fairing, and a horizon-sensor fairing. The schematics of all protuberances and their orientation with the basic model are shown in Fig. 4. The left-side auxiliary-equipment fairing (Fig. 4d) was equipped with either a conical or wedge afterbody, whereas the right-side auxiliary-equipment fairing (Fig. 4e) incorporated either a blunt or conical afterbody.

Configuration 1 was comprised of all the protuberances with the 10-deg cone and blunt afterbody installed on the left- and right-side auxiliary-equipment fairings, respectively. Configuration 2 was identical to Configuration 1 with the exception of an 8-deg wedge and a 20-deg cone installed on the left- and right-side auxiliary-equipment fairings, respectively. Configuration 3 evolved from Configuration 2 by removing the right-side auxiliary-equipment fairing. Likewise, Configuration 4 was Configuration 2 with the horizon-sensor fairing removed. Table I, Appendix II, gives a detailed listing of the protuberances that comprise each configuration. Installation photographs of Configurations 1, 2, 3, and 4 are shown in Fig. 5.

A sketch of the boundary-layer rakes (typical) that were used on all configurations is shown in Fig. 6. Rake (A) was located directly behind the P_1 fin and thruster module combination at model station 37.2. Rake (B) was located at the same model station but displaced -45 deg along the model circumference. Both rakes are shown installed on the model in Fig. 3.

2.3 INSTRUMENTATION

The model steady-state instrumentation consists of 84 static-pressure taps and 22 total-pressure probes. The total-pressure probes were from two boundary-layer rakes of 11 tubes each. A total of one hundred and six 15-psid transducers were used to measure the steady-state pressure levels. The locations of all static- and dynamic-pressure taps and ports in respect to the model are shown in Fig. 7.

Forty-two flush-mounted microphones were used to measure unsteady pressures on the model surface. The output signals from these

microphones were conditioned by miniature preamplifiers mounted within the model in proximity to the microphones. The output signals were recorded on magnetic tape. Two accelerometers were also located inside the model to give an indication of the vibration level. The signals from the accelerometers were also recorded on magnetic tape. Microphone locations are also shown in Fig. 7.

A schlieren system was used to obtain still pictures of the flow about the model.

SECTION III
PROCEDURE

3.1 GENERAL

All configurations were tested at Mach numbers from 0.80 through 1.55 at total pressures from 1800 to 2350 psf. The variation of tunnel unit Reynolds number with Mach number for the test is given in Fig. 8. Configurations 1 and 2 were tested at angles of attack from -7.5 to 4 deg at 0-deg roll angle; 6 and -6 deg at 90-deg roll angle; and 0 deg at 64- and 116-deg roll angle. Configuration 3 remained at 0-deg angle of attack and 116-deg roll angle throughout the entire Mach number range. The angle of attack remained at 0 deg with roll angle at 64 and 116 deg for Configuration 4.

Steady-pressure data along with schlieren photographs were obtained for all test conditions. Fluctuating-pressure data were obtained at all test conditions except at 64- and 116-deg roll angle for Configurations 1 and 2.

3.2 PRECISION OF MEASUREMENTS

The uncertainties in setting and maintaining tunnel conditions are estimated to be as follows:

Free-stream Mach number	±0.005
Free-stream total pressure	±5 psf
Total temperature	±5°F
Angle of attack	±0.1 deg
Roll angle	±0.1 deg

SECTION IV
RESULTS AND DISCUSSION

4.1 GENERAL

Determining the steady- and fluctuating-pressure levels around flow-perturbing geometries required considerable static- and dynamic-pressure instrumentation near and aft of the protuberances of interest. Of prime interest was the influence on the fluctuating-pressure levels resulting from various afterbody geometries on the two (left- and right-side) auxiliary-equipment fairings.

For presentation purposes, the rows of microphones were numbered 1, 2, 3, and 4 as noted in Fig. 7. Figure 9 shows the variation of the ratio of the fluctuating pressure level (rms) of each microphone to the local static-pressure level along each row as functions of free-stream Mach number and model station. Figure 10 shows corresponding static-pressure levels for each row of microphones for Configurations 1 and 2.

The data from microphones designated A31, A32, A24, and A25 in rows 1, 2, 3, and 4, respectively, were selected for further comparison. Local dynamic-pressure ratios for microphones A31, A32, A24, and A25 were determined by ratioing the root-mean-square value of the dynamic pressure at A31 and A32 to P80 and P81, respectively, and A24 and A25 to P54. The values of local static pressure used for each test condition are shown in Tables II and III for the model at ϕ = 0 and 90 deg, respectively.

4.2 INTERFERENCE EFFECTS, α_m = 0

Before making a valid comparison of the afterbodies in Configurations 1 and 2, it was deemed necessary to examine the mutual interference of the afterbodies as well as the interference on the afterbodies from other protuberances.

The variation of local dynamic-pressure ratios as functions of free-stream Mach number for Configurations 1, 2, 3, and 4 for microphones A31, A32, A24, and A25 is shown in Fig. 11. All data shown were recorded at α_m = 0 deg; however, the roll angles were ϕ = 0 deg for Configurations 1 and 2, 116 deg for Configuration 3, and 64 deg for Configuration 4. Configuration 3 is the same as Configuration 2, except that the entire right-side auxiliary-equipment fairing and its 20-deg conical

afterbody have been removed (Fig. 5d). The local fluctuating pressure-ratio levels at microphones A31 and A32 at all Mach numbers for Configuration 3 are approximately the same as for Configuration 2. Apparently the effect of the right-side auxiliary-equipment fairing and its afterbodies on microphones A31 and A32 is not significant.

Configuration 4, which is the same as Configuration 2 with the horizon-sensor fairing removed (Fig. 5e), exhibited lower fluctuating-pressure-ratio levels at microphone A31 than were experienced with Configuration 2 for Mach numbers above 1.2. This indicates that at M_∞ = 1.55 at the A31 location, approximately 0.0179 or 50 percent of the local fluctuating pressure could be attributable to the influence of the horizon-sensor fairing, located approximately 64 deg around, and 12 in. (model scale) forward of A31. This effect of the horizon-sensor fairing on A31 should be considered when evaluating the level of local dynamic-pressure ratio at M_∞ = 1.55 for Configurations 1 and 2. No data were available for A32 for Configuration 4.

When the right-side auxiliary-equipment fairing was removed (Configuration 3) the local dynamic-pressure ratio of A24 decreased significantly from the levels experienced during Configuration 2 testing in the supersonic speed range. However, when the auxiliary-equipment fairing was replaced and the horizon-sensor fairing was removed (Configuration 4), the level of the local dynamic-pressure ratio increased only slightly over that obtained for Configuration 3. The only difference in model geometry from Configuration 2 to Configuration 4 was the removal of the horizon sensor. It appears that a large part of the local dynamic-pressure fluctuations experienced at microphone A24 with either afterbody installed was caused, in part, by the interaction of the flow fields from the right-side auxiliary-equipment fairing and from the horizon-sensor fairing.

The most severe local pressure fluctuations occurred at the location of microphone A25. Note that at the location of A25, removing the horizon-sensor fairing (Configuration 4) had the effect of increasing the local dynamic-pressure ratio level compared to the pressure-ratio levels experienced during the Configuration 2 testing, which is a reversal of the effect of removing this protuberance on A31 and A24.

4.3 EVALUATION OF FAIRING AFTERBODY CONFIGURATIONS 1 AND 2

Configurations 1 and 2 were tested at angle-of-attack settings of -7.5, 0, and 4 deg over the Mach number range from 0.80 to 1.55 at

ϕ = 0 deg. Local dynamic-pressure ratios as a function of Mach number, configuration, and angle of attack are shown in Fig. 12.

Replacing the 10-deg cone (Configuration 1) with the 8-deg wedge afterbody (Configuration 2) on the left-side auxiliary-equipment fairing had almost negligible effect on the local dynamic-pressure ratio at microphones A31 and A32. Dynamic-pressure levels were slightly higher for Configuration 2 than for Configuration 1 at the higher Mach numbers.

The dynamic pressures from microphones A24 and A25 indicate that replacing the blunt afterbody (Configuration 1) with the 20-deg cone (Configuration 2), on the right-side auxiliary-equipment fairing, generally had the effect of decreasing the dynamic-pressure levels for the corresponding pitch angles up to Mach number 1.4; however, this relationship was reversed for some pitch angles at Mach numbers 1.10, 1.20, and 1.55. It is not obvious why the pressure ratio at microphone A25 decreases abruptly at M_∞ = 1.55 for Configuration 1, but the results indicate that the level of dynamic-pressure fluctuations is not greatly affected by the afterbody geometry at M_∞ = 1.55. The 10-deg conical afterbody exhibited the lowest overall dynamic-pressure level of the four afterbodies at all test conditions.

Sideslipping the model ±6 deg appears to have a negligible effect on the local dynamic-pressure ratios for microphones A31 and A32 for each configuration over the Mach number range tested (Fig. 13). Microphones A31 and A32 exhibited slightly higher levels of dynamic pressure for Configuration 2 than for Configuration 1 at Mach numbers greater than 1.2.

Neither Configuration 1 or 2 caused the dynamic-pressure level to be consistently higher than the other at microphone A24. The most significant difference in pressure ratio occurred at M_∞ = 1.55 when Configuration 2 showed higher fluctuation for both sideslip angles than did Configuration 1.

The microphone A25 data indicate that a significant decrease in dynamic-pressure ratio resulted when the blunt base was replaced with the conical afterbody for Mach numbers up to 1.4. The data trend at M_∞ = 1.55 leads to the same conclusion reached previously that the blunt afterbody has about the same effect as the conical afterbody on the dynamic pressure at microphone A25. It would appear from the trend of these data (as well as from Figs. 11 and 12) that at $M_\infty > 1.55$, the blunt afterbody may impose lower dynamic-pressure loads at A25 than those imposed by the 20-deg conical afterbody.

SECTION V
CONCLUSIONS

With the data obtained from selected microphones of the MOL fluctuating-pressure model, the following conclusions can be made:

1. The left-side and right-side auxiliary-equipment fairings and their afterbodies do not impose a significant interference effect on each other.
2. The horizon-sensor-fairing and auxiliary-equipment-fairing flow interaction accounts for up to 50 percent of the pressure fluctuations of microphones A24 and A32 at the higher Mach numbers.
3. The 10-deg conical afterbody exhibited the lowest overall dynamic-pressure level of the four afterbodies, at all test conditions.

REFERENCES

1. Test Facilities Handbook (Seventh Edition). "Propulsion Wind Tunnel Facility, Vol. 5." Arnold Engineering Development Center, July 1968.
2. Gunn, J. A. "Check Calibration of the AEDC 16-Ft Transonic Tunnel." AEDC-TR-66-80 (AD633277), May 1966.
3. Riddle, C. D. "Investigation of Free-Stream Fluctuating Pressures in the 16-Ft Tunnels of the Propulsion Wind Tunnel Facility." AEDC-TR-67-167 (AD818388), August 1967.

APPENDIXES

I. ILLUSTRATIONS

II. TABLES

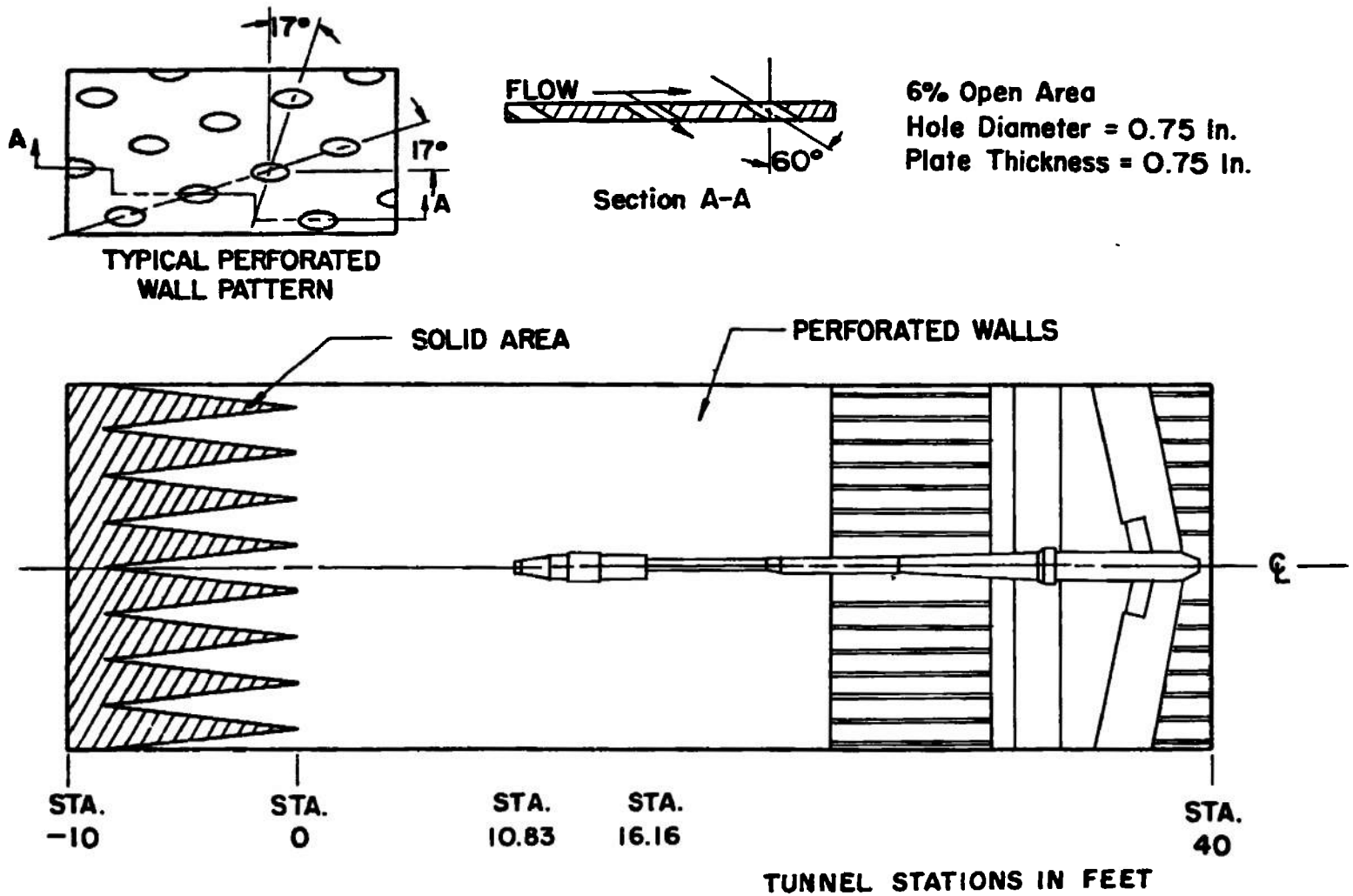

Fig. 1 Schematic of the MOL Fluctuating-Pressure Model in 16T Test Section

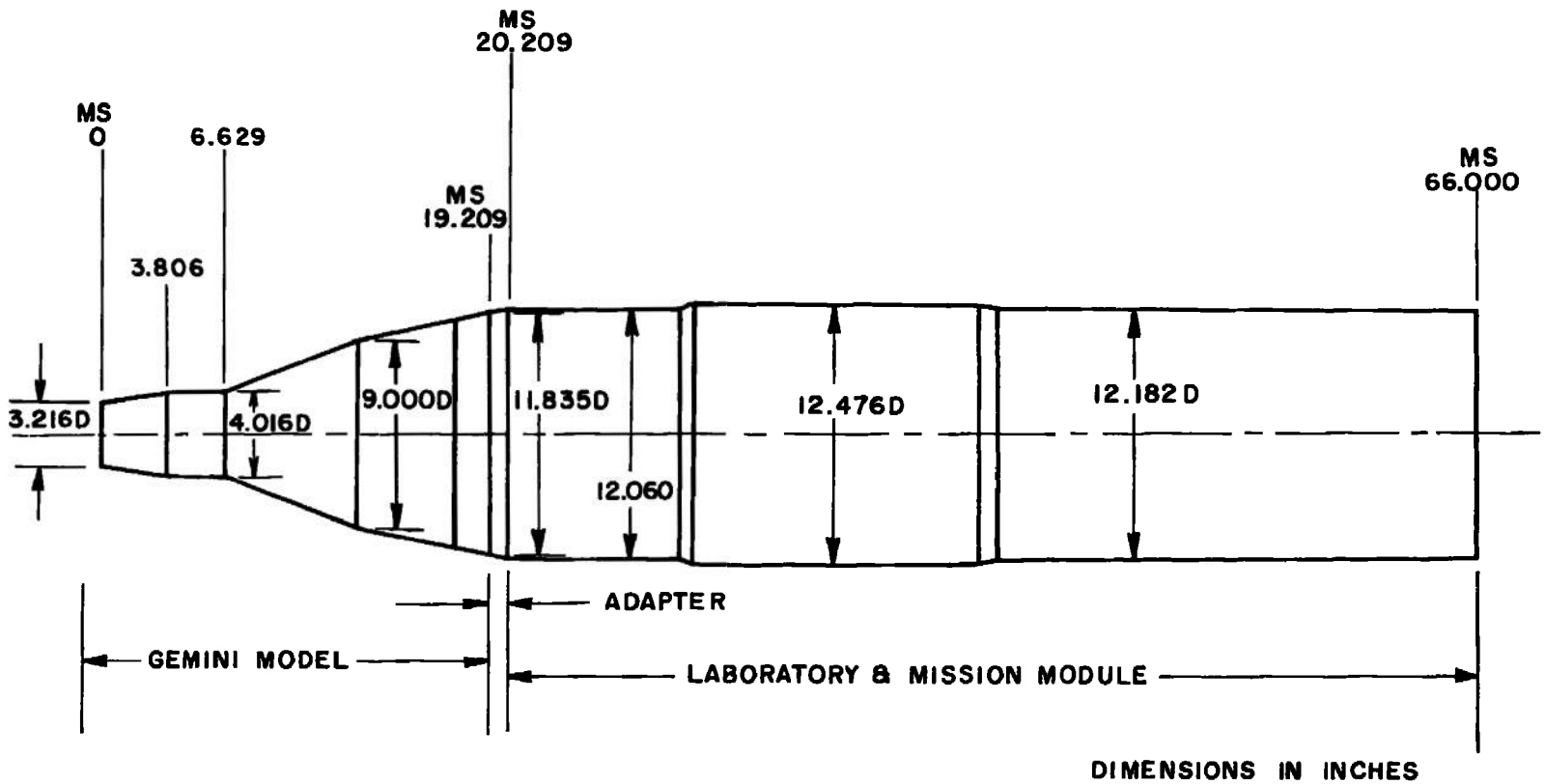

Fig. 2 Basic Model Configuration

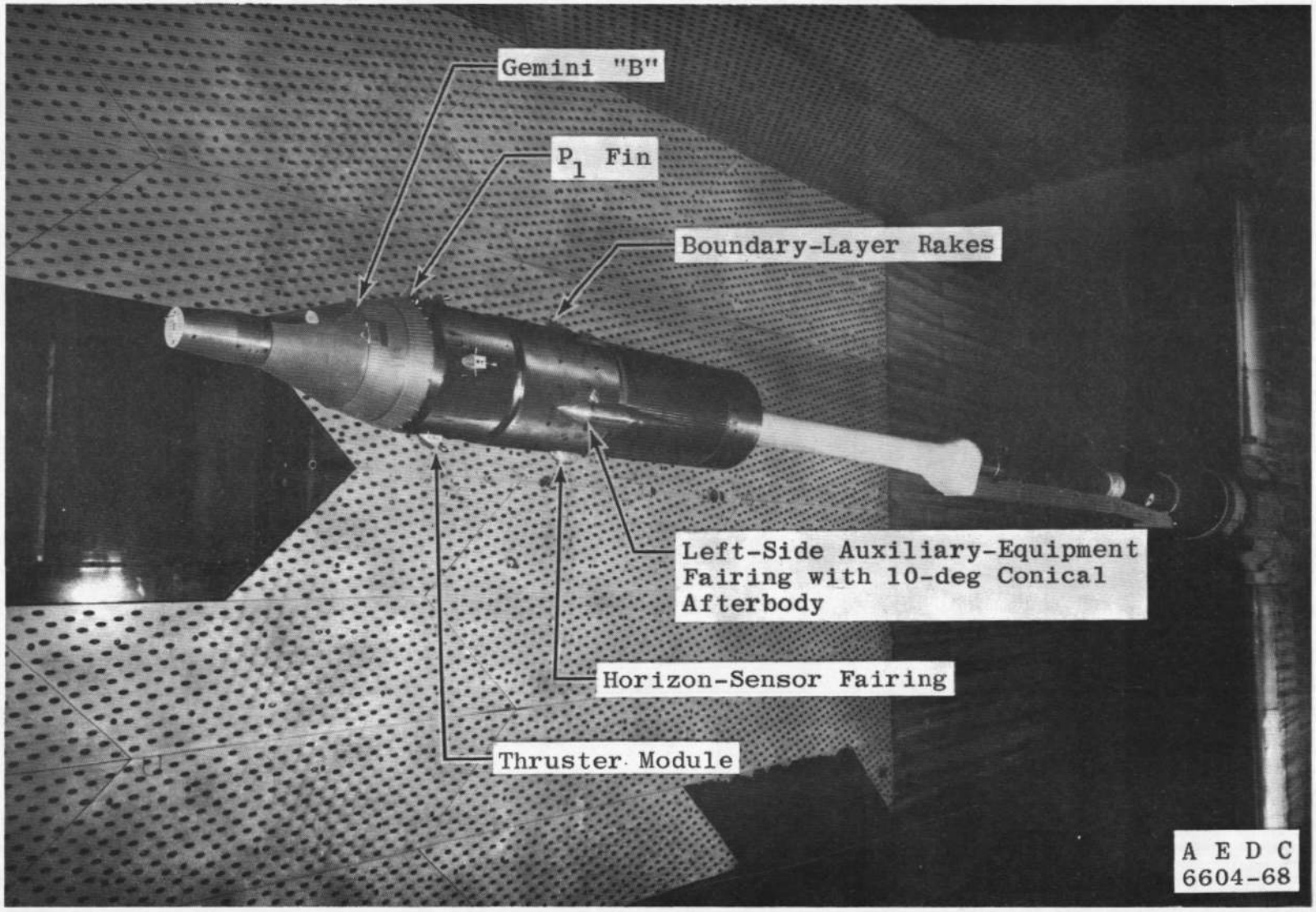

Fig. 3 Configuration 1 Installed in the Test Section

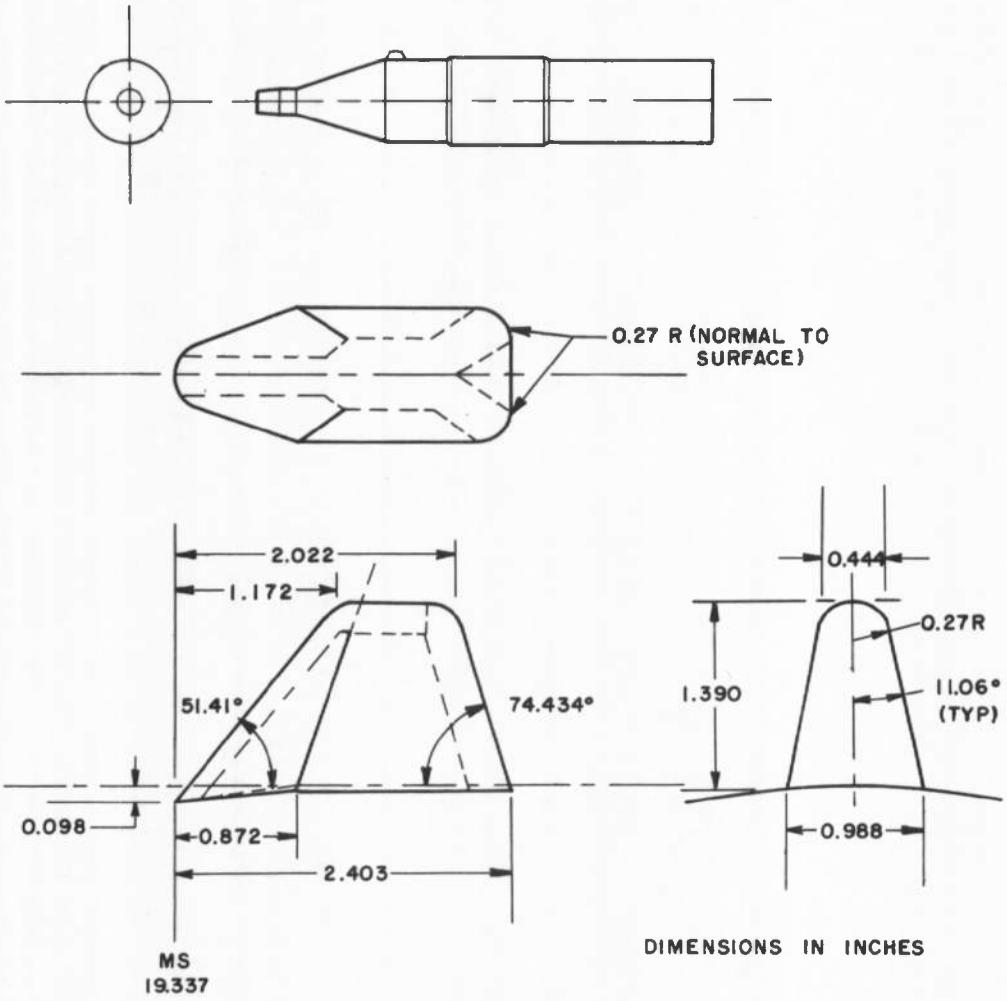

a. P_1 Fin

Fig. 4 Model Protuberances

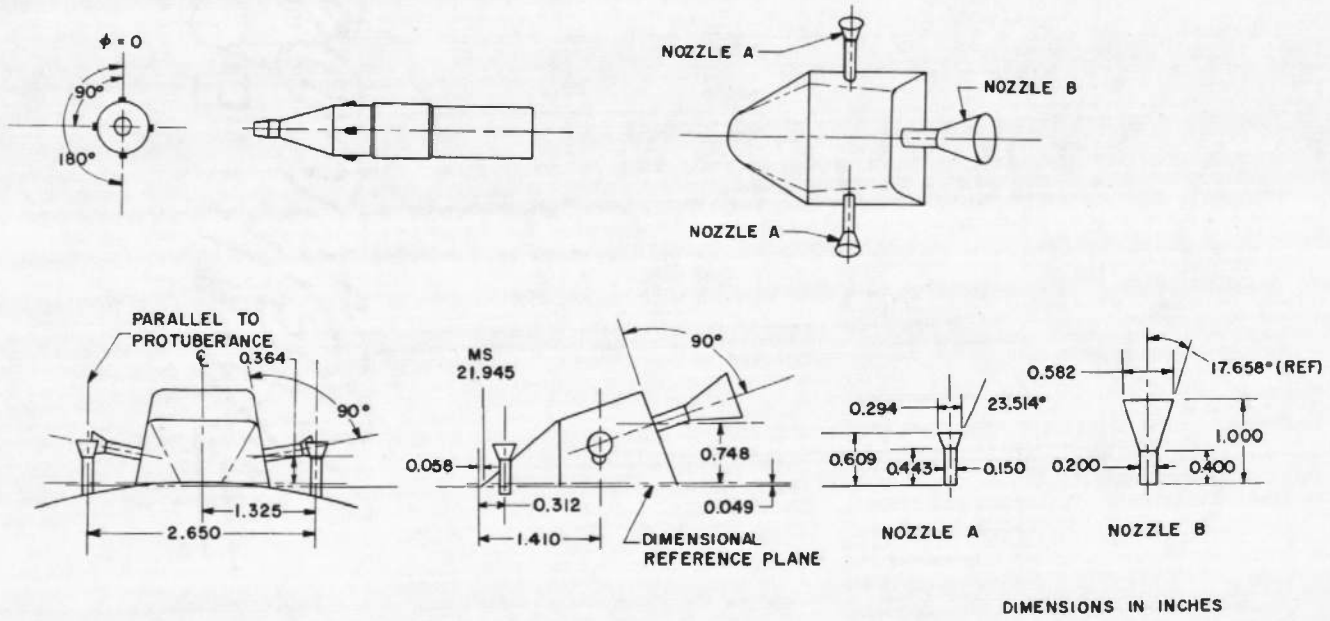

b. Thruster Module

Fig. 4 Continued

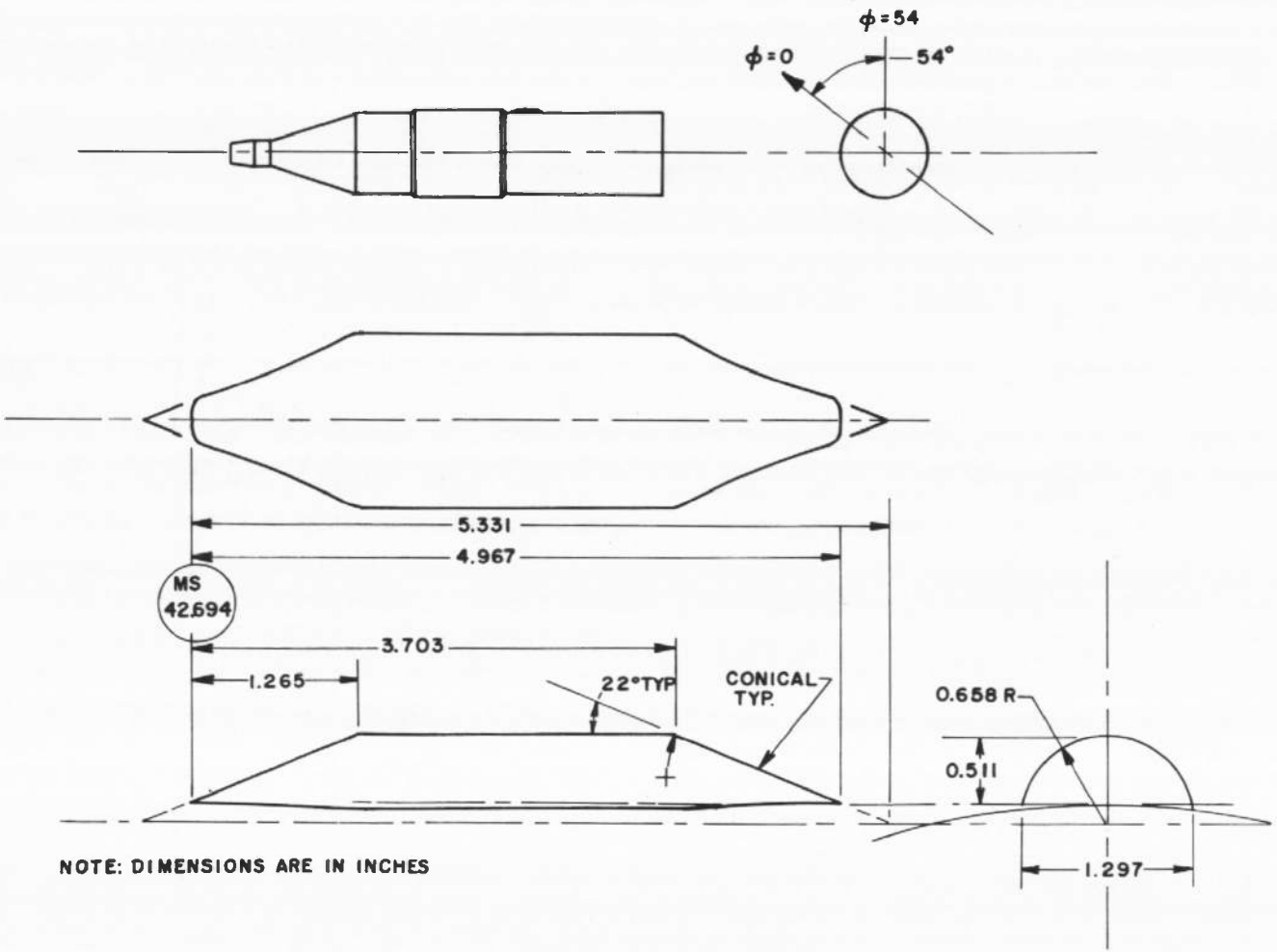

c. Mission-Module Foiring

Fig. 4 Continued

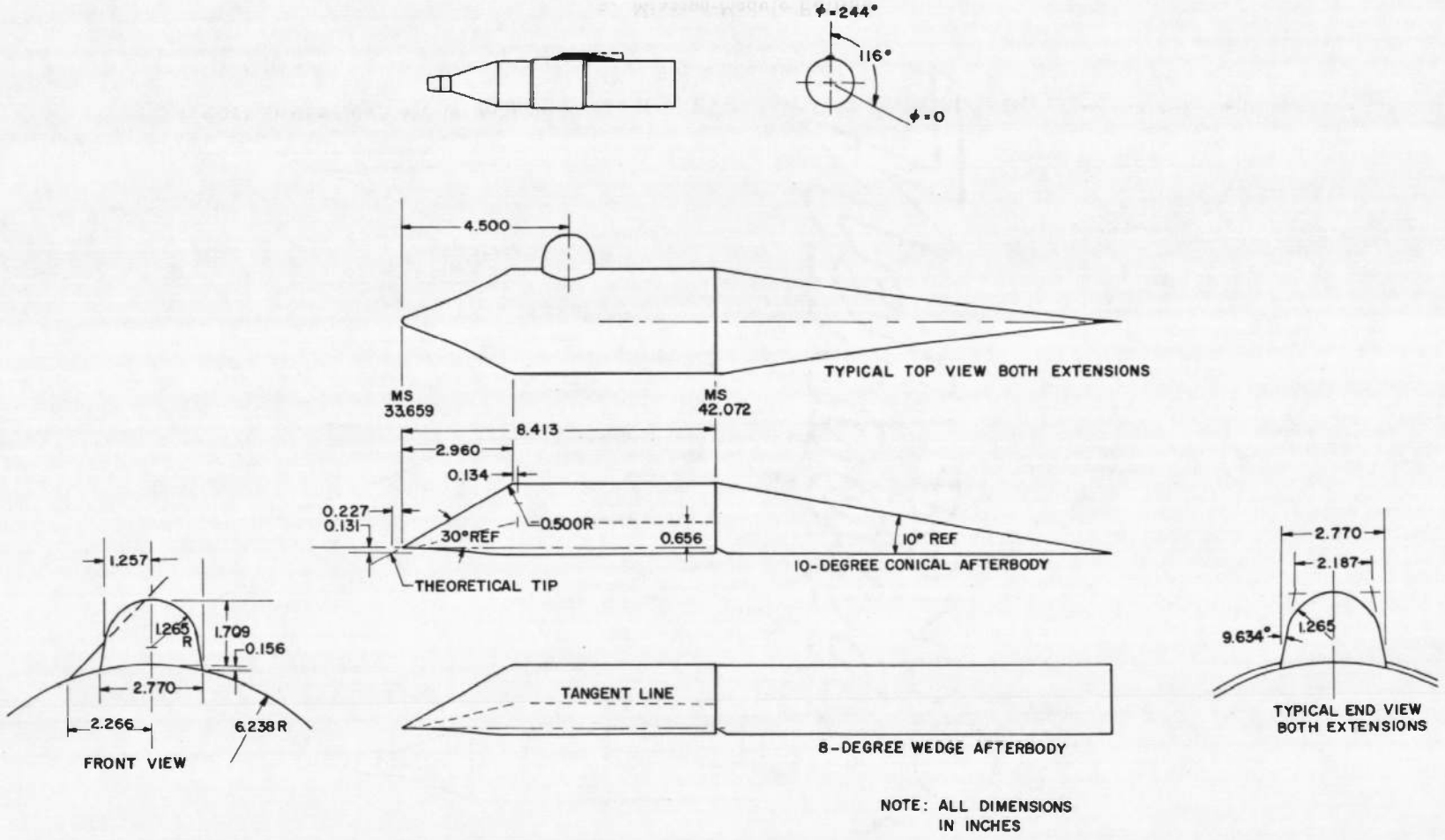

d. Left-Side Auxiliary-Equipment Fairing with 10-deg Cone and 8-deg Wedge Afterbody

Fig. 4 Continued

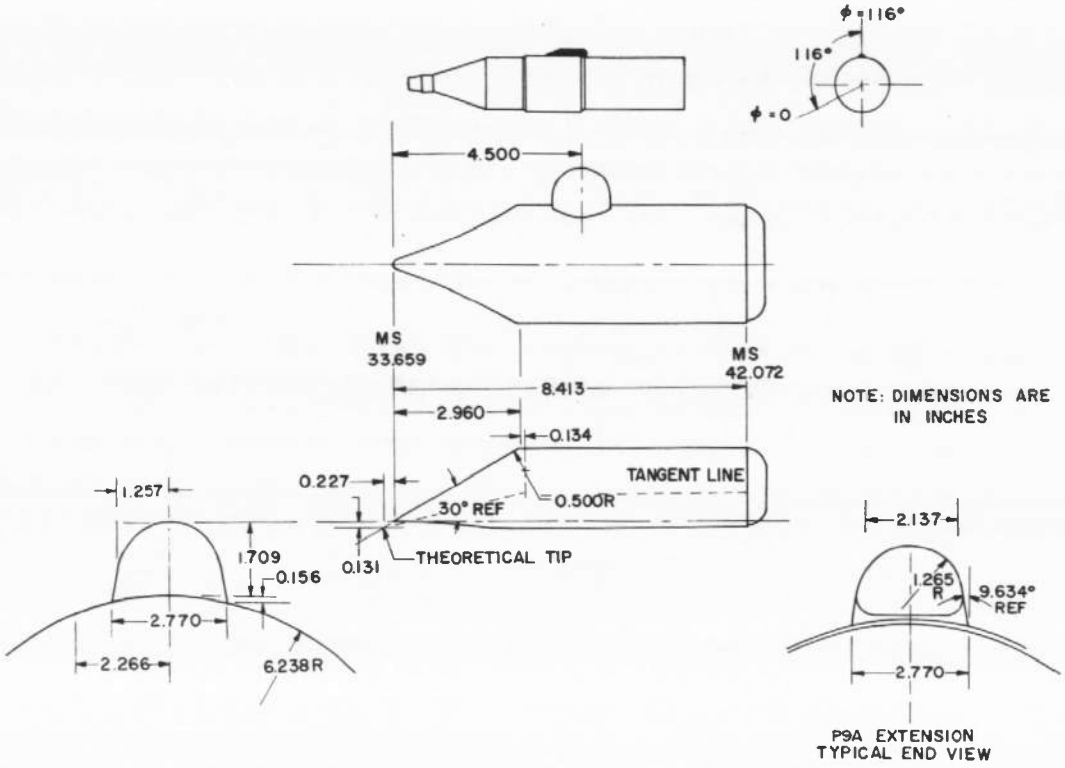

e. Right-Side Auxiliary-Equipment Fairing with Blunt Base
Fig. 4 Continued

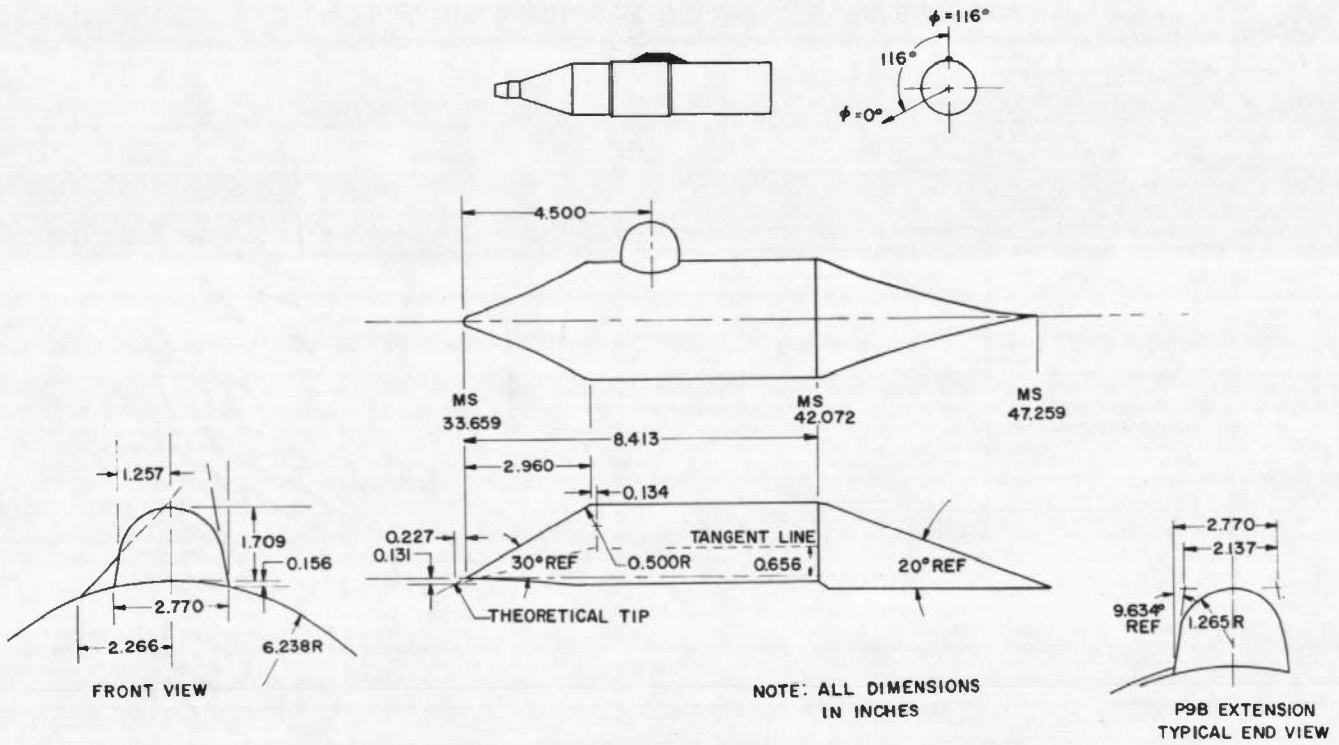

f. Right-Side Auxiliary-Equipment Fairing with 20-deg Conical Afterbody

Fig. 4 Continued

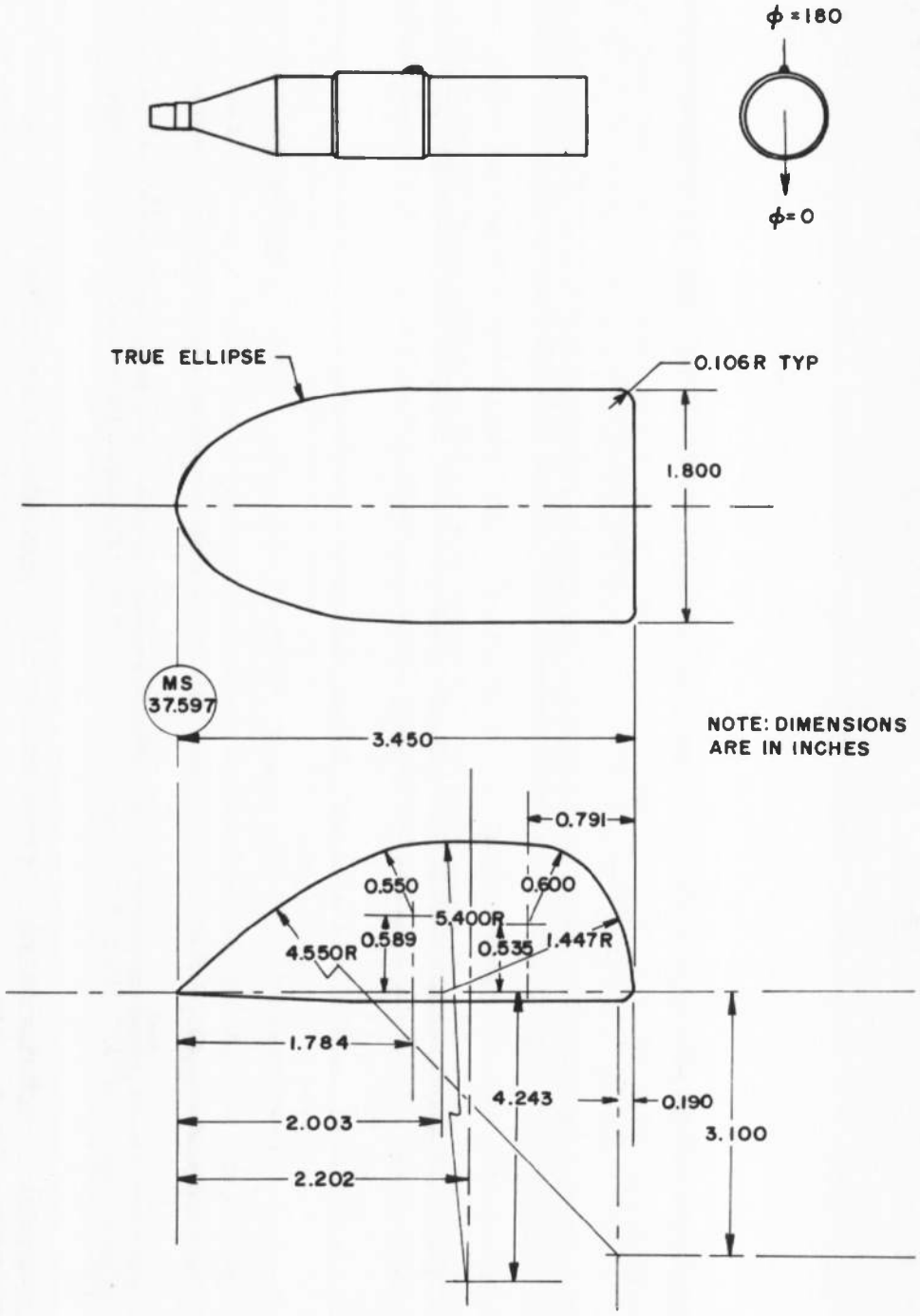

g. Horizon-Sensor Fairing
Fig. 4 Concluded

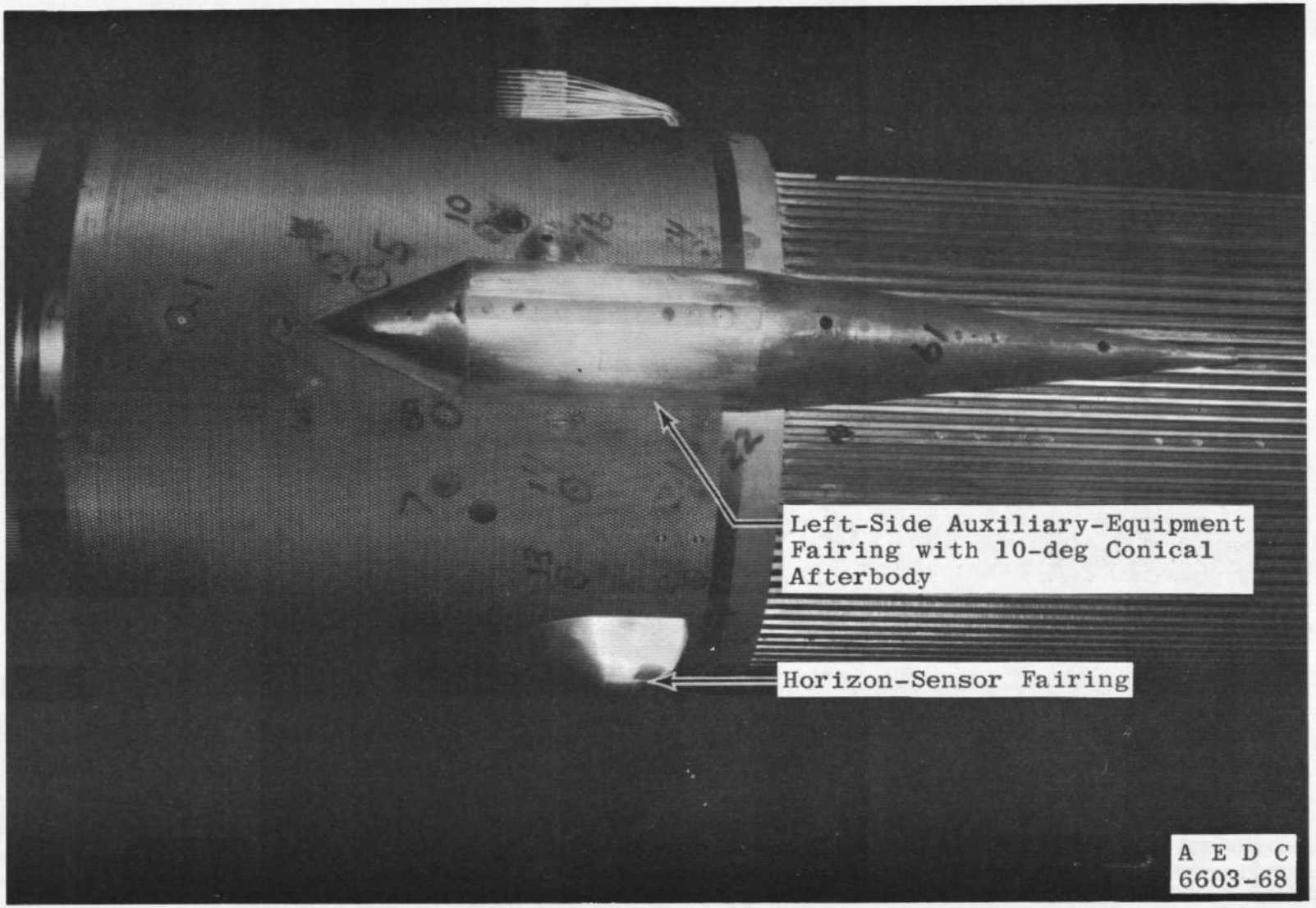

a. Configuration 1, 10-deg Conical Afterbody on Left-Side Auxiliary-Equipment Fairing

Fig. 5 Configuration Photographs

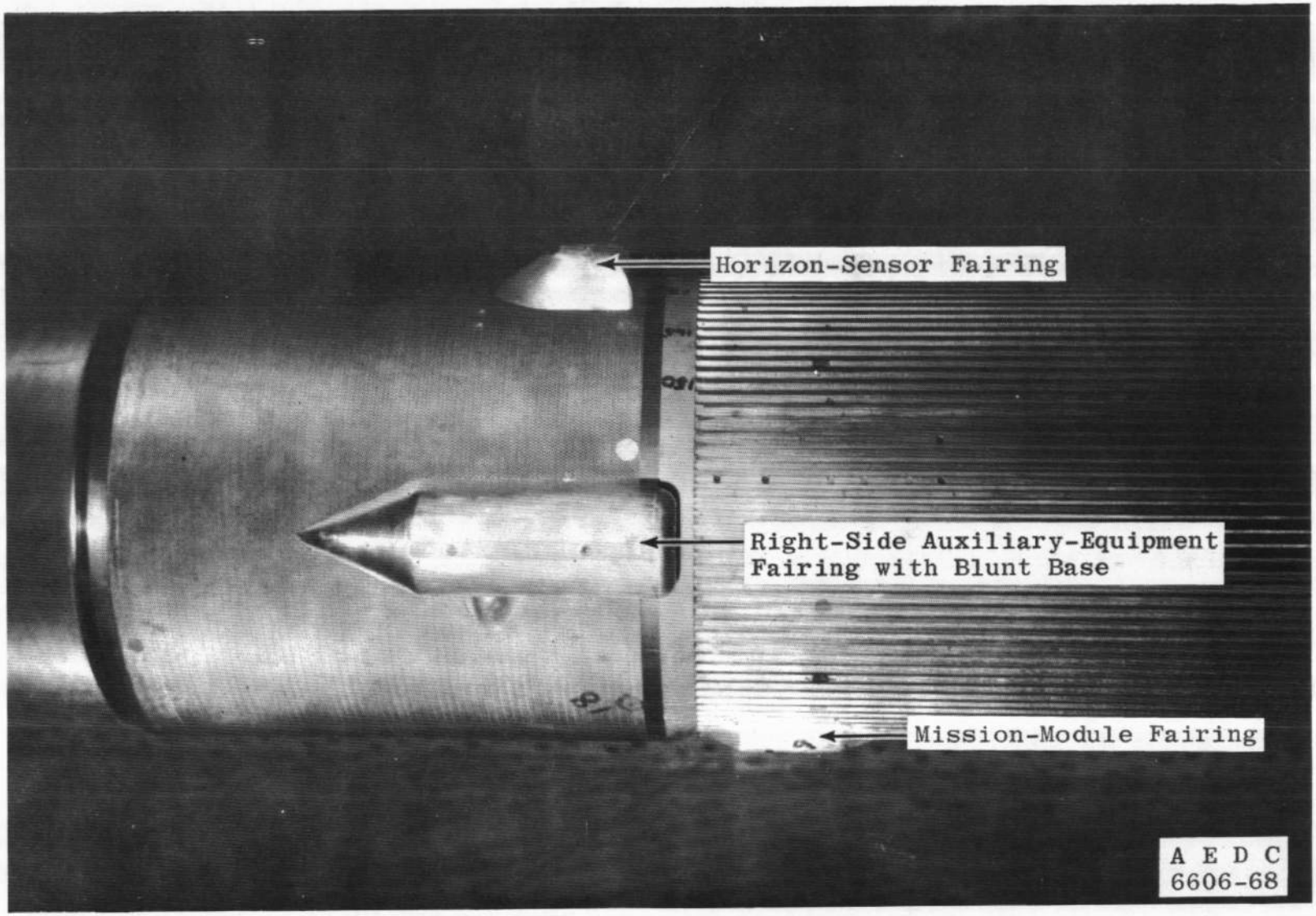

b. Configuration 1, Blunt Base on Right-Side Auxiliary-Equipment Fairing

Fig. 5 Continued

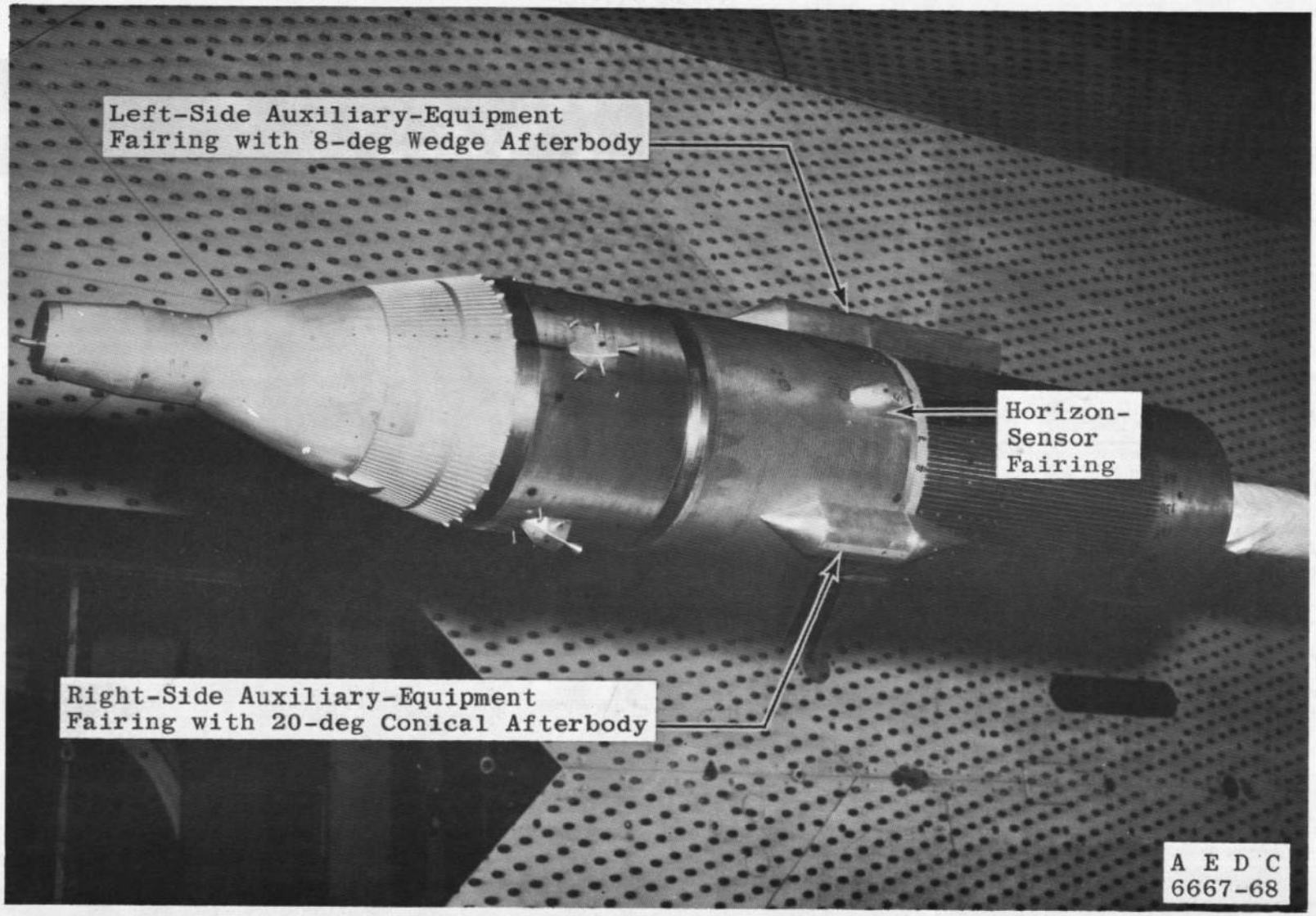

c. Configuration 2, 20-deg Cone and 8-deg Wedge Afterbody on Right- and Left- Side Auxiliary-Equipment Fairing, Respectively

Fig. 5 Continued

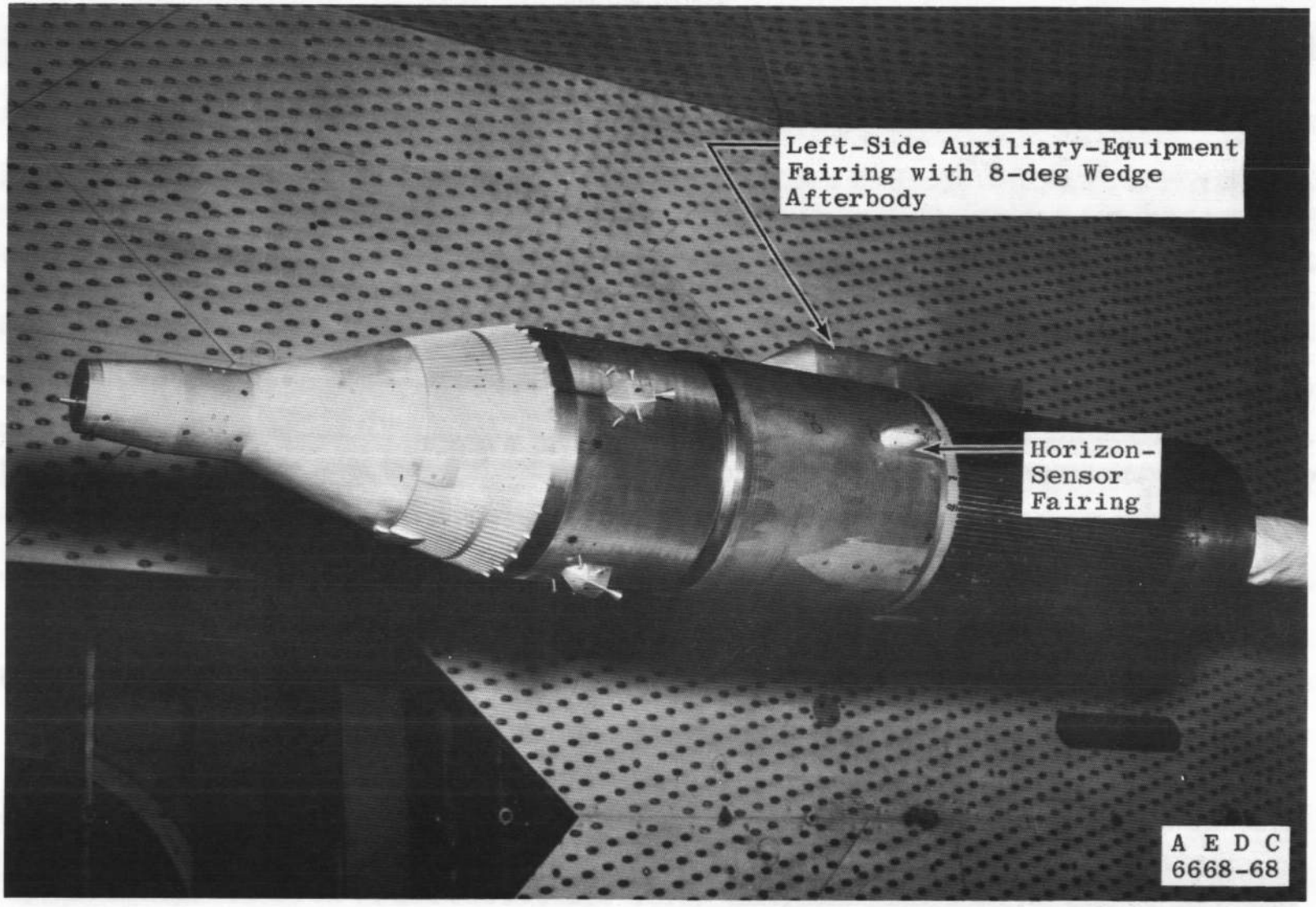

d. Configurotion 3, Right-Side Auxiliary-Equipment Fairing Removed

Fig. 5 Continued

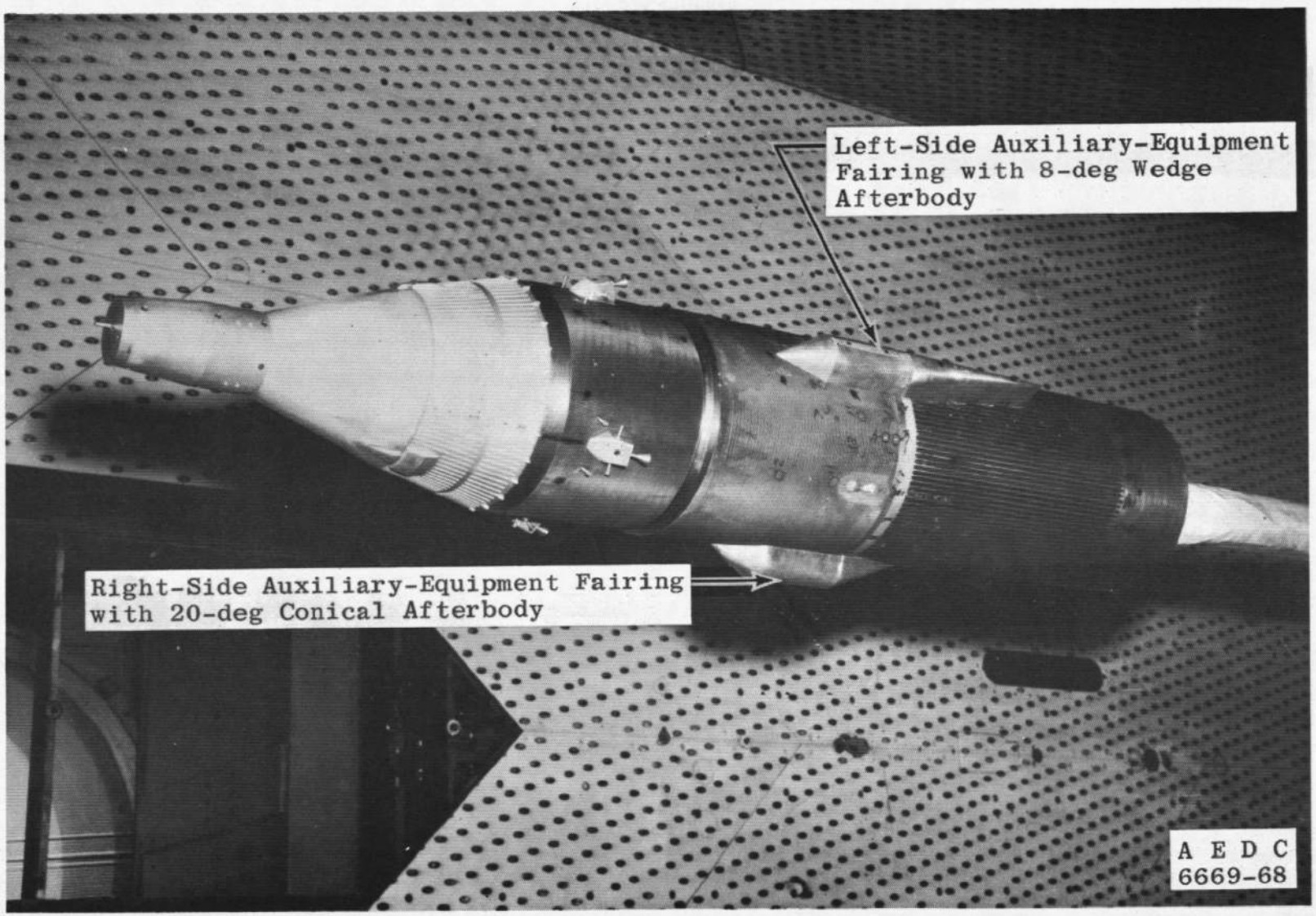

e. Configuration 4, Horizon-Sensor Removed

Fig. 5 Concluded

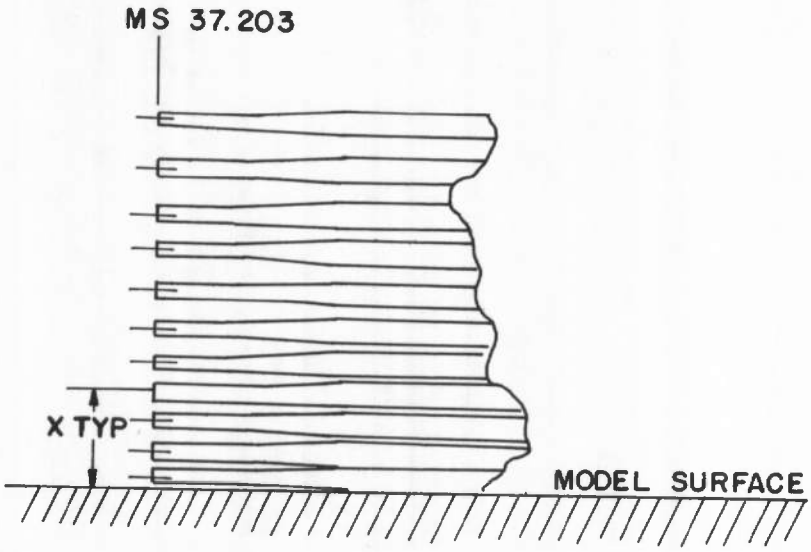

TUBE NUMBER SYSTEM		
X (INCH)	RAKE AT $\phi = 0$	RAKE AT $\phi = 315$
1.000	111	122
0.870	110	121
0.750	109	120
0.640	108	119
0.535	107	118
0.435	106	117
0.340	105	116
0.255	104	115
0.175	103	114
0.100	102	113
0.030	101	112

Fig. 6 Schematic of Boundary-Layer Rake

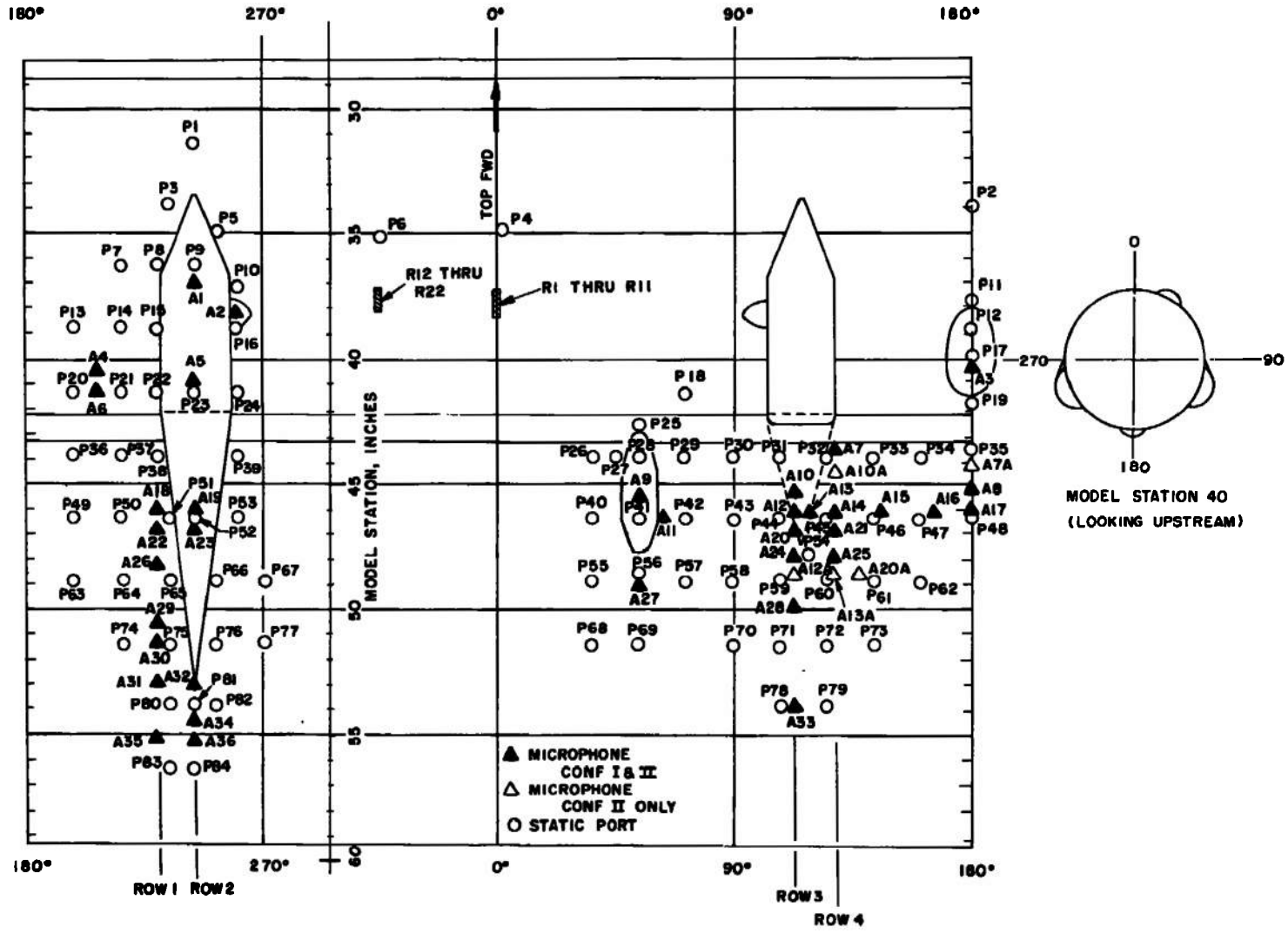

Fig. 7 Static- and Dynamic-Pressure Port Locations

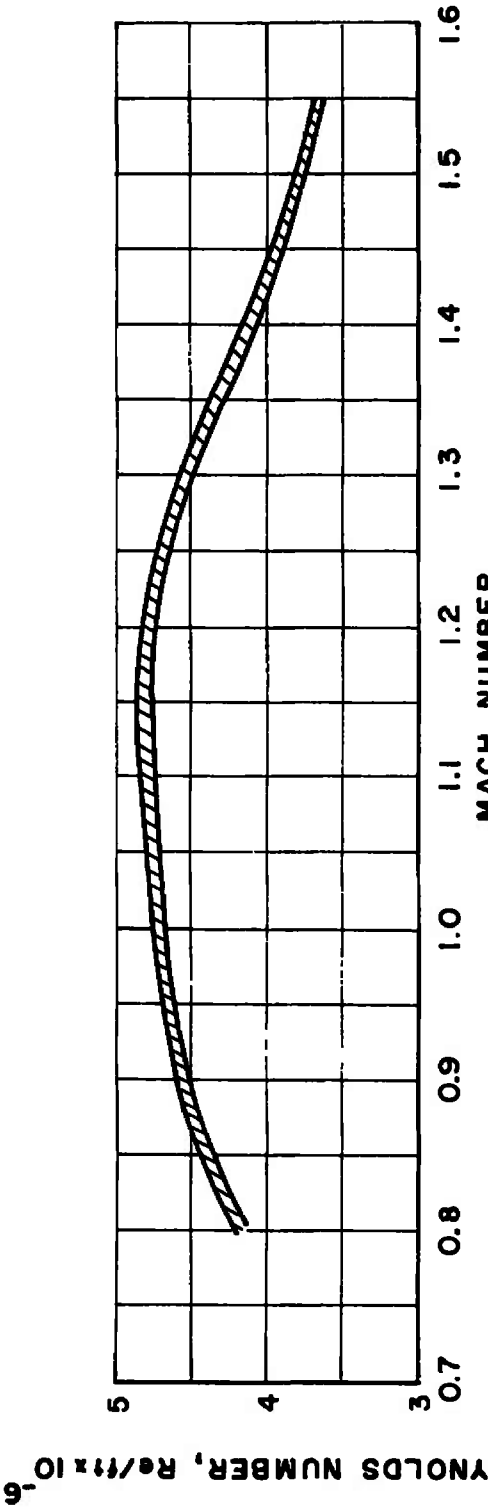

Fig. 8 Variation of Tunnel Unit Reynolds Number with Mach Number

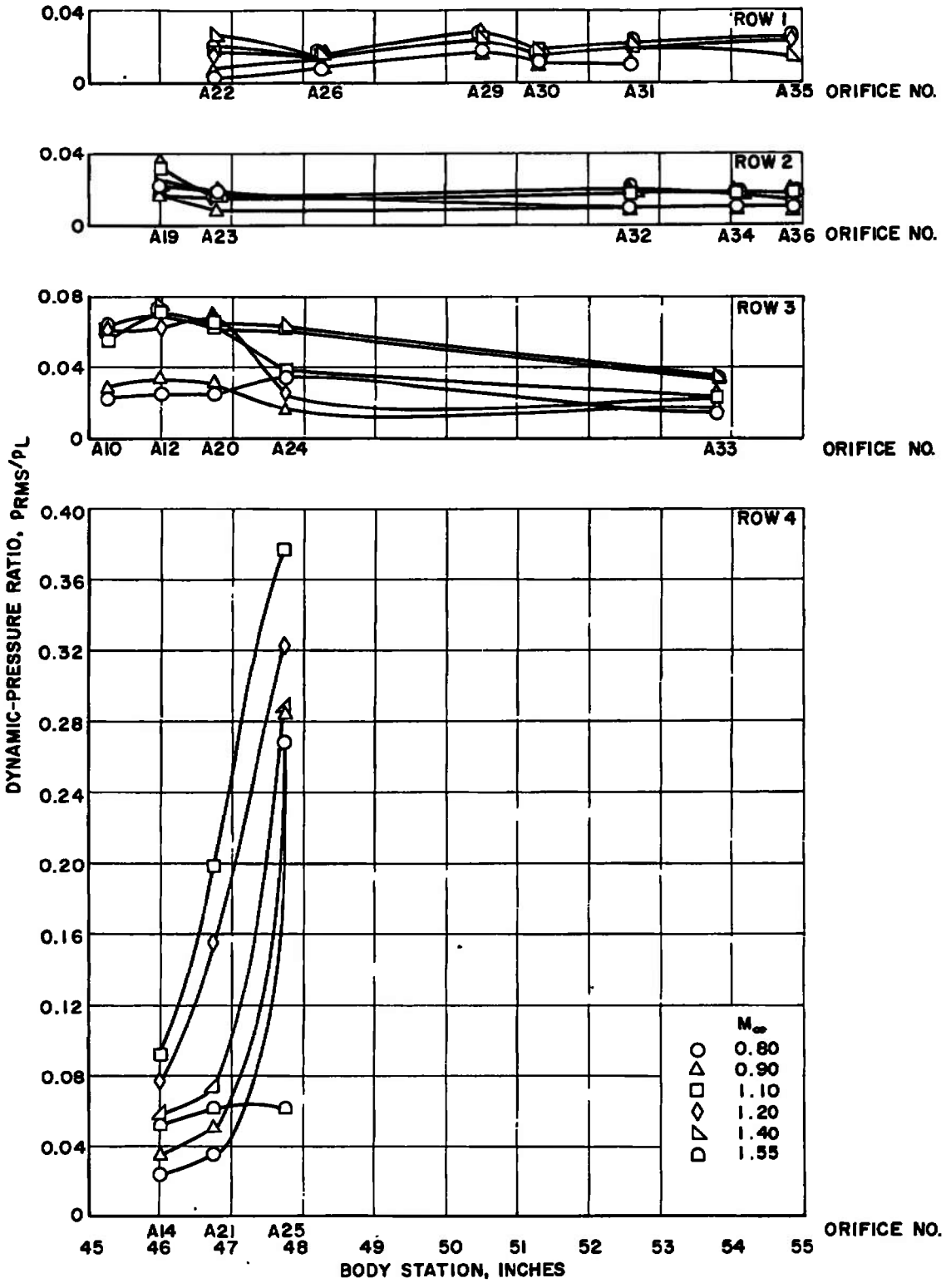

a. Configuration 1

Fig. 9 Variation of Local Dynamic-Pressure Ratio with Model Body Station, $\alpha_m = 0$, $\phi = 0$

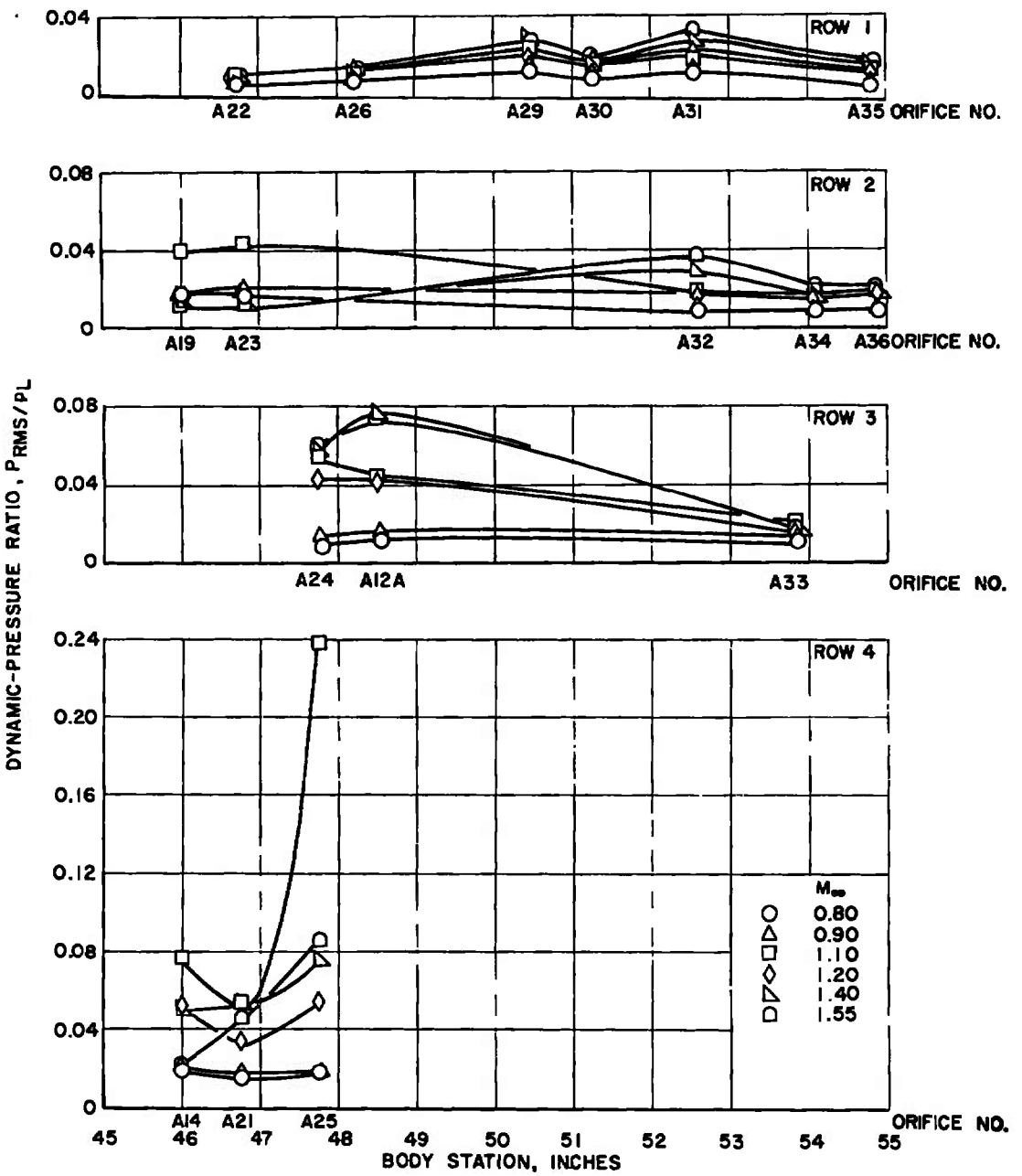

b. Configuration 2

Fig. 9 Concluded

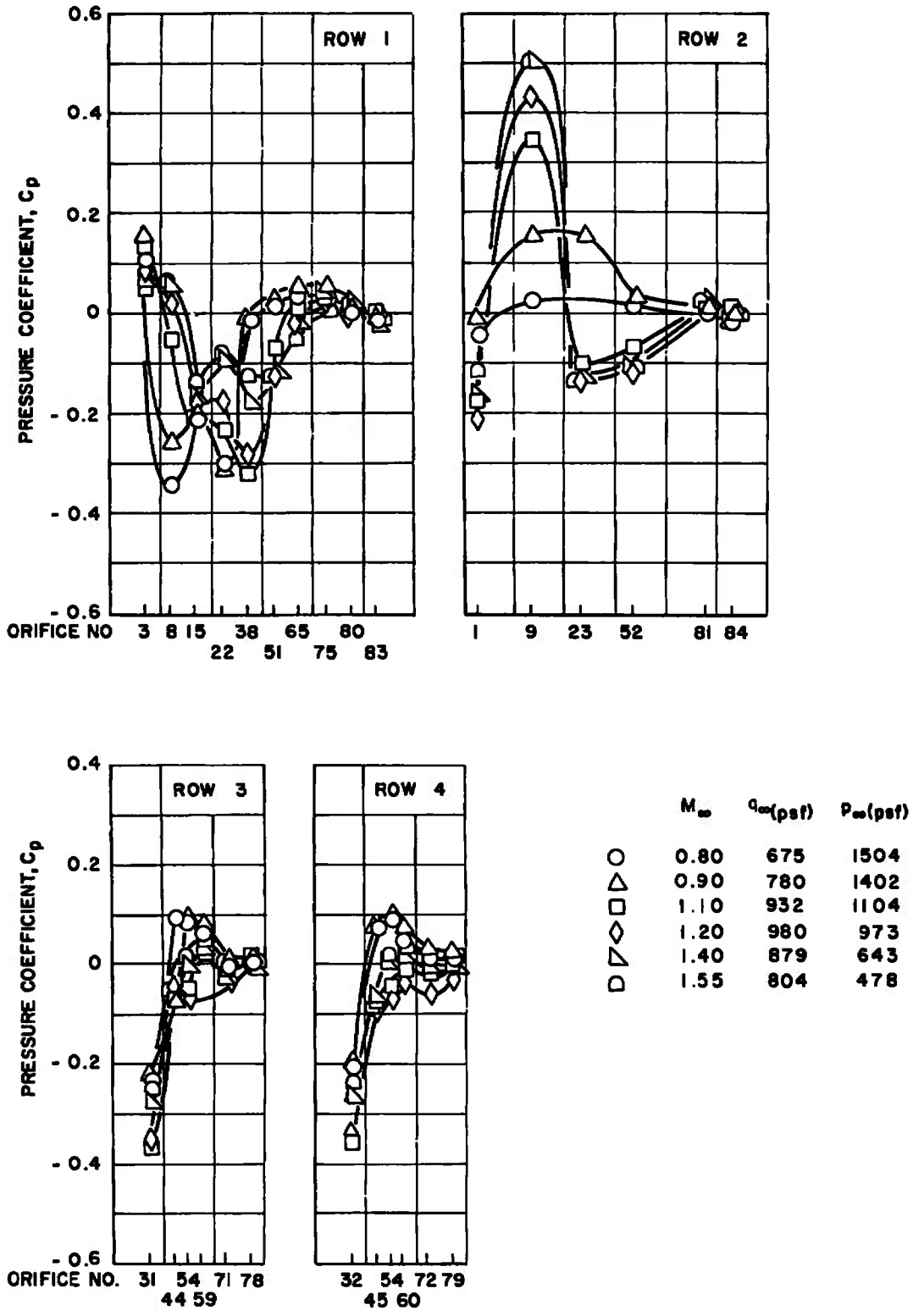

a. Configuration 1

Fig. 10 Variation of Local Pressure Coefficient with Model Orifice Number

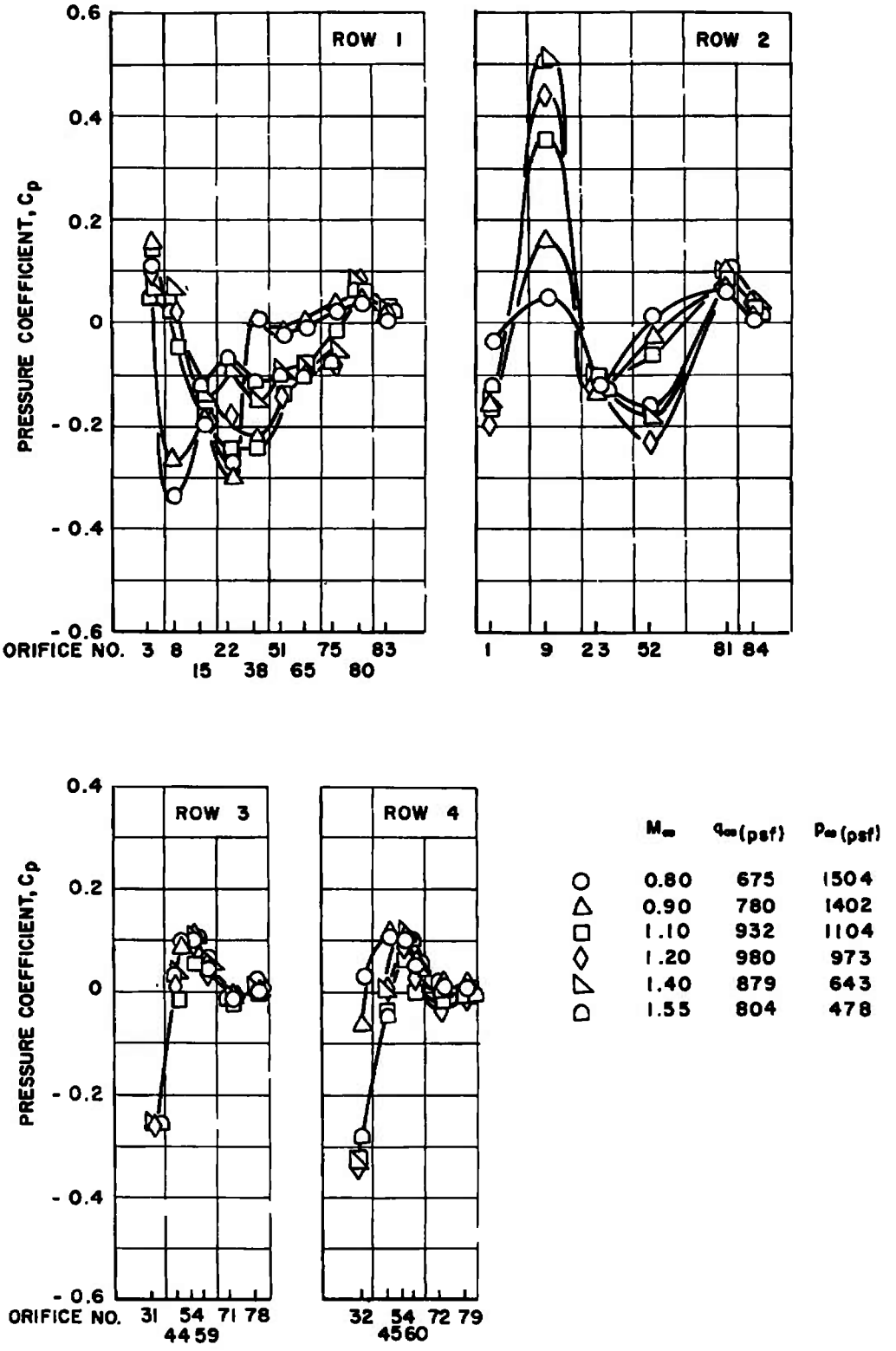

b. Configuration 2

Fig. 10 Concluded

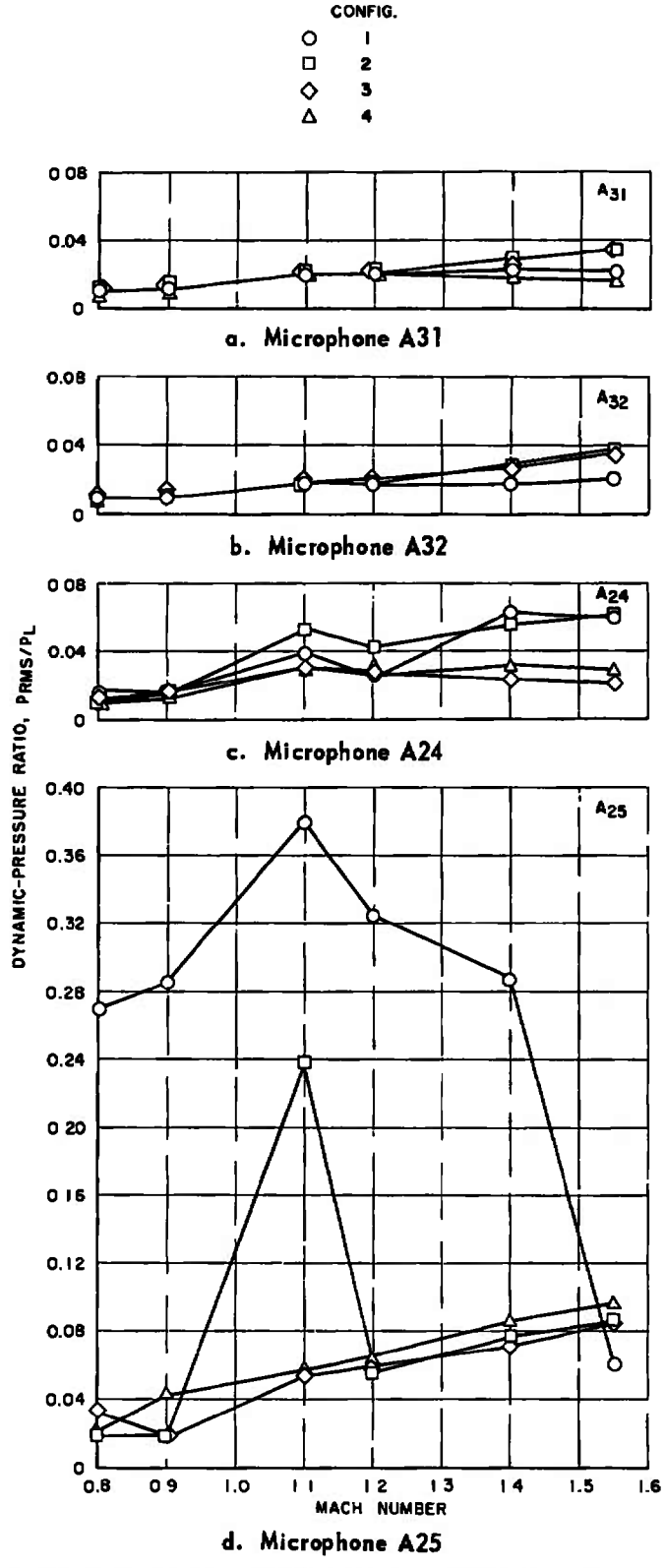

Fig. 11 Variation of Local Dynamic-Pressure Ratio with Mach Number for Configurations 1, 2, 3, and 4, $\alpha_m = 0$

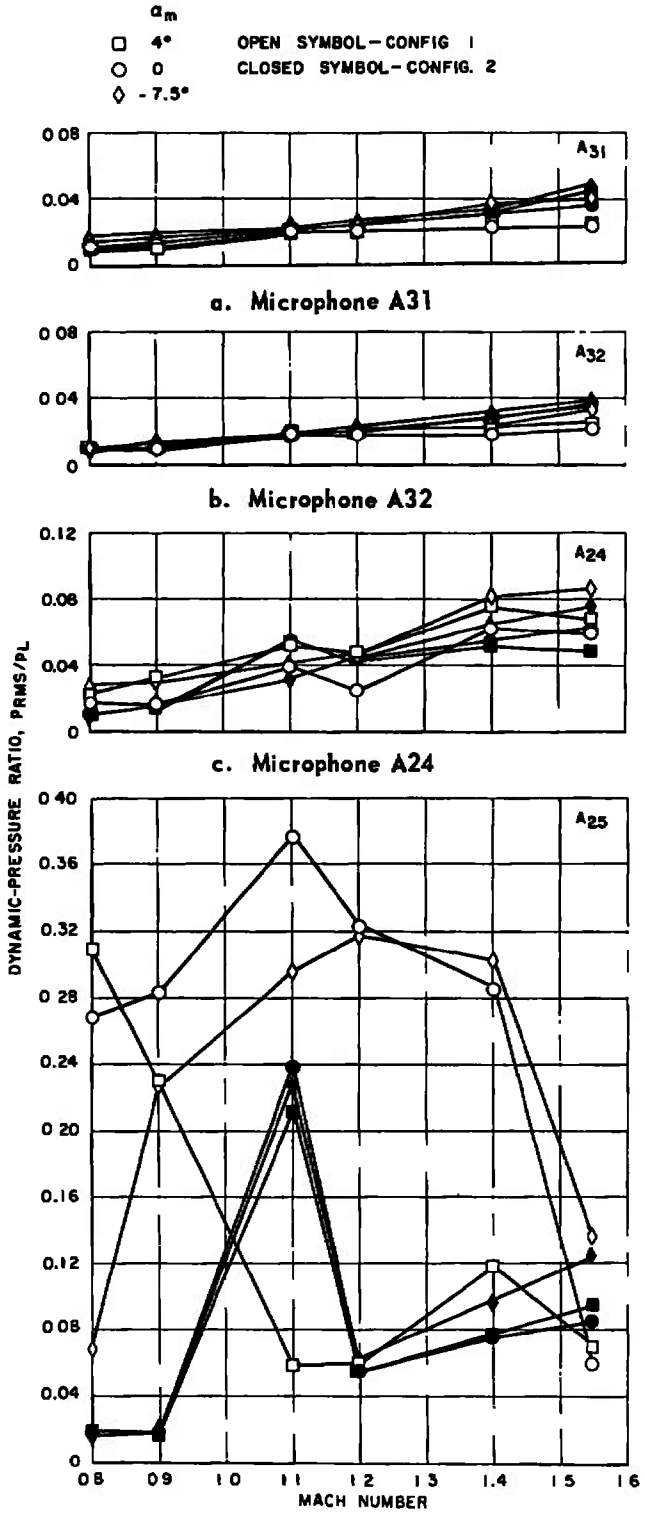

a. Microphone A31

b. Microphone A32

c. Microphone A24

d. Microphone A25

Fig. 12 Variation of Local Dynamic-Pressure Ratio with Mach Number and Model Angle of Attack for Configurations 1 and 2

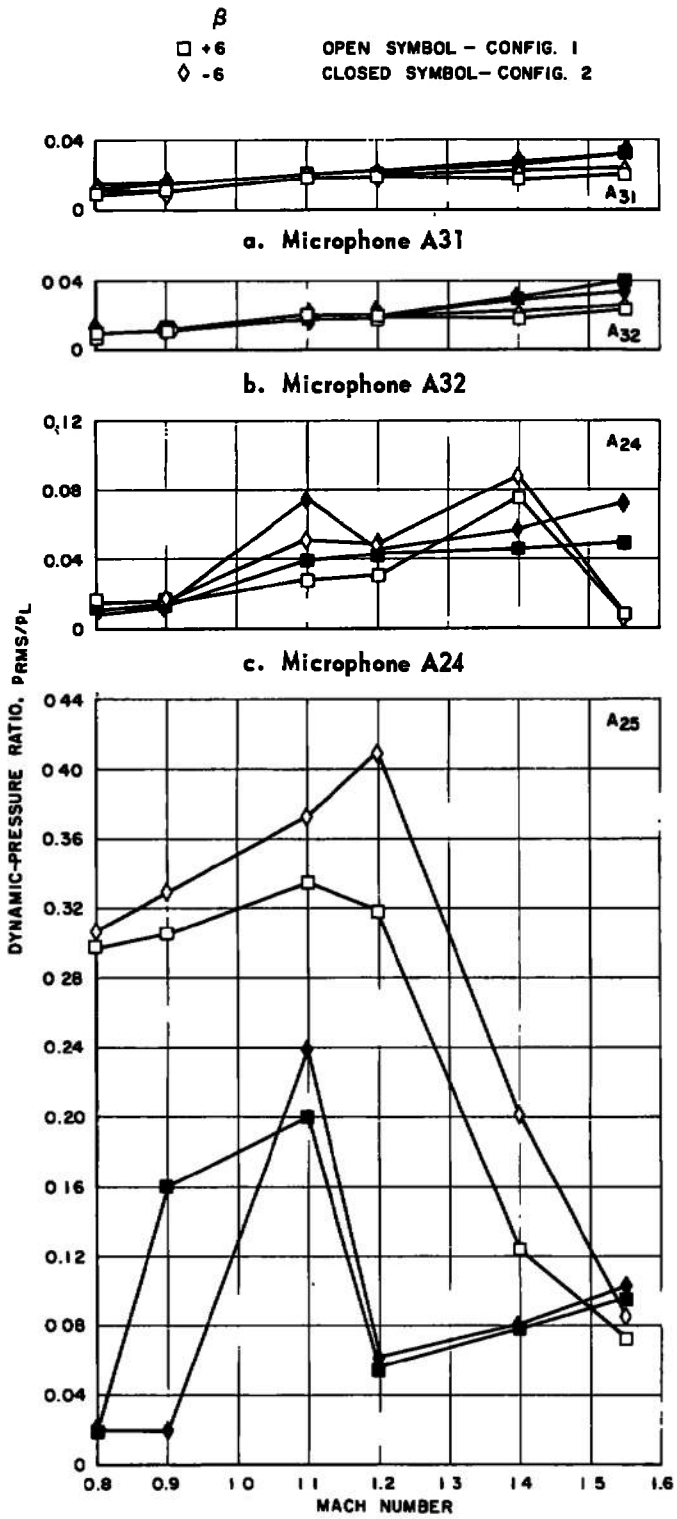

Fig. 13 Variation of Local Dynamic-Pressure Ratio with Mach Number and Model Sideslip for Configurations 1 and 2

TABLE I
MODEL CONFIGURATIONS

Protuberances	Config. 1	Config. 2	Config. 3	Config. 4
P_1 fin	x	x	x	x
Four thruster modules	x	x	x	x
Mission-module fairing	x	x	x	x
Left-side auxiliary-equipment fairing with 10-deg conical afterbody	x			
Left-side auxiliary-equipment fairing with 8-deg wedge afterbody		x	x	x
Right-side auxiliary-equipment fairing with blunt afterbody	x			
Right-side auxiliary-equipment fairing with 20-deg conical afterbody		x		x
Horizon-sensor fairing	x	x	x	

TABLE II
REFERENCE PRESSURES FOR MICROPHONES A31, A32, A24, A25 PRESSURE RATIOS AT MODEL ROLL ANGLE, 0 DEG

Config.	Point No.	M_∞	α, deg	p80, psf (Microphone A31)	p81, psf (Microphone A32)	p54, psf (Microphones A24 and A25)
1	2/1	0.80	-7.5	1479	1481	1478
	2/2		0	1510	1510	1559
	2/3		4.0	1510	1514	1516
	3/5	0.90	4.0	1409	1414	1447
	3/6		0	1417	1416	1476
	3/7		-7.5	1379	1383	1371
	4/1	1.10	-7.5	1076	1085	1013
	4/2		0	1125	1126	1062
	4/3		4.0	1112	1115	1009
	5/5	1.20	4.0	978	985	896
	5/6		0	990	993	902
	5/7		-7.5	922	935	861
	8/1	1.40	-7.5	584	607	527
	8/2		0	668	670	640
	8/3		4.0	664	679	641
	12/1	1.55	-7.5	418	423	378
	12/2		0	497	502	492
	12/3		4.0	465	478	476
2	15/1	0.80	-7.5	1507	1518	1532
	15/3		0	1534	1548	1573
	15/4		4.0	1529	1550	1572
	16/5	0.90	4.0	1442	1469	1504
	16/6		0	1443	1460	1489
	16/7		-7.5	1392	1408	1428
	17/1	1.10	-7.5	1111	1129	1090
	17/2		0	1153	1174	1145
	17/3		4.0	1152	1189	1167
	18/5	1.20	4.0	1000	1049	1056
	18/6		0	1036	1063	1045
	18/7		-7.5	947	961	928
	19/1	1.40	-7.5	679	663	612
	19/2		0	712	734	736
	19/3		4.0	673	725	743
	20/4	1.55	4.0	473	548	553
	20/5		0	518	552	550
	20/6		-7.5	446	507	461

TABLE III
REFERENCES PRESSURES FOR MICROPHONES A31, A32, A24, AND A25
PRESSURE RATIOS AT MODEL ROLL ANGLE, 90 DEG

Config.	Point No.	M_∞	α, deg	p80, psf (Microphone A31)	p81, psf (Microphone A32)	p54, psf (Microphones A24 and A25)
1	2/5	0.80	6	1507	1513	1579
	2/6		-6	1519	1521	1519
	3/2	0.90	-6	1417	1416	1413
	3/3		6	1395	1399	1495
	4/5	1.10	6	1113	1118	1133
	4/6		-6	1118	1119	1016
	5/2	1.20	-6	983	986	823
	5/3		6	968	972	1003
	8/5	1.40	6	634	638	662
	8/6		-6	670	667	558
	12/5	1.55	6	455	458	474
	12/6		-6	488	485	411
2	15/6	0.80	6	1521	1542	1585
	15/7		-6	1558	1564	1571
	16/2	0.90	-6	1470	1483	1478
	16/3		6	1422	1446	1510
	17/5	1.10	6	1146	1177	1186
	17/6		-6	1189	1196	1090
	18/2	1.20	-6	1049	1057	969
	18/3		6	1003	1038	1058
	19/5	1.40	6	664	701	749
	19/6		-6	730	726	697
	20/2	1.55	-6	545	542	515
	20/3		6	491	526	575

UNCLASSIFIED

Security Classification

DOCUMENT CONTROL DATA - R & D

(Security classification of title, body of abstract and indexing annotation must be entered when the overall report is classified)

1 ORIGINATING ACTIVITY *(Corporate author)*
Arnold Engineering Development Center
ARO, Inc., Operating Contractor
Arnold Air Force Station, Tenn. 37389

2a. REPORT SECURITY CLASSIFICATION
UNCLASSIFIED

2b. GROUP
N/A

3 REPORT TITLE
STEADY AND FLUCTUATING PRESSURES AROUND FLOW PROTUBERANCES ON THE MOL VEHICLE AT TRANSONIC SPEEDS

This document has been approved for public release its distribution is unlimited. Per TAB 74-6 dtd 15 March 74

4 DESCRIPTIVE NOTES *(Type of report and inclusive dates)*
Final Report July 2 to 9, 1968

5 AUTHOR(S) *(First name, middle initial, last name)*
R. W. Butler and J. F. Riddell, ARO, Inc.

6 REPORT DATE	7a. TOTAL NO OF PAGES	7b. NO. OF REFS
September 1968	45	3

8a. CONTRACT OR GRANT NO	9a. ORIGINATOR'S REPORT NUMBER(S)
F40600-69-C-0001	AEDC-TR-68-203
b. Program Element 6340940F/632A	
c.	9b. OTHER REPORT NO(S) *(Any other numbers that may be assigned this report)*
d	N/A

10 DISTRIBUTION STATEMENT This document may be further distributed by any holder only with specific prior approval of SAMSO (SMSDI-STINFO), AF Unit Post Office, Los Angeles, California 90045.

11 SUPPLEMENTARY NOTES	12 SPONSORING MILITARY ACTIVITY
Available in DDC.	SAMSO (SMSDI-STINFO) AF Unit Post Office Los Angeles, California 90045

13 ABSTRACT

A wind tunnel investigation was conducted in the Propulsion Wind Tunnel, Transonic (16T) to obtain steady and fluctuating pressures to assess the aerodynamic effects on the local and downstream flow fields caused by large protuberances on the Manned Orbital Laboratory (MOL) vehicle. Pressure data were recorded at Mach numbers 0.80, 0.90, 1.10, 1.20, 1.40, and 1.55 for angles of attack of -7.5, 0, and 4 deg and angles of sideslip of -6 and 6 deg. Test results revealed that the left- and right-side auxiliary-equipment fairings and their afterbodies do not impose a significant interference effect on each other, whereas the horizon-sensor-fairing and auxiliary-equipment-fairing flow interaction attributes up to 50 percent of the pressure fluctuations at selected microphone locations. Of the four base configurations on the auxiliary-equipment fairings, the 10-deg conical afterbody exhibited the lowest overall dynamic-pressure level at all test conditions.

This document may be further distributed by any holder only with specific prior approval of SAMSO (SMSDI-STINFO), AF Unit Post Office, Los Angeles, California 90045.

DD FORM 1 NOV 65 1473

UNCLASSIFIED

Security Classification

14. KEY WORDS	LINK A ROLE	LINK A WT	LINK B ROLE	LINK B WT	LINK C ROLE	LINK C WT
Manned Orbital Laboratory						
protuberances, effects of						
pressure measurements						
transonic flow						
wind tunnel testing						

2. Protuberances

4. Space vehicles -- Protuberances

5. " " -- Pressure distribution

6. " " -- Transonic flow

19-4.